2016

Adenosine A1 receptor protects against cisplatin ototoxicity by suppressing the NOX3/STAT1 inflammatory pathway in the cochlea

Tejbeer Kaur
Washington University School of Medicine

Vikrant Borse
Southern Illinois University School of Medicine

Sandeep Sheth
Southern Illinois University School of Medicine

Kelly Sheehan
Southern Illinois University School of Medicine

Sumana Ghosh
Southern Illinois University School of Medicine

See next page for additional authors

Cellular/Molecular

Adenosine A_1 Receptor Protects Against Cisplatin Ototoxicity by Suppressing the NOX3/STAT1 Inflammatory Pathway in the Cochlea

Tejbeer Kaur,[1]* Vikrant Borse,[2]* Sandeep Sheth,[2] Kelly Sheehan,[3] Sumana Ghosh,[2] Srinivasan Tupal,[2] Sarvesh Jajoo,[2] Debashree Mukherjea,[3] Leonard P. Rybak,[2,3] and Vickram Ramkumar[2]

[1]Department of Otolaryngology, Washington University School of Medicine, St. Louis, Missouri 63110, and [2]Department of Pharmacology and [3]Department of Surgery, Southern Illinois University School of Medicine, Springfield, Illinois 62794

Cisplatin is a commonly used antineoplastic agent that produces ototoxicity that is mediated in part by increasing levels of reactive oxygen species (ROS) via the NOX3 NADPH oxidase pathway in the cochlea. Recent studies implicate ROS generation in mediating inflammatory and apoptotic processes and hearing loss by activating signal transducer and activator of transcription (STAT1). In this study, we show that the adenosine A_1 receptor (A_1AR) protects against cisplatin ototoxicity by suppressing an inflammatory response initiated by ROS generation via NOX3 NADPH oxidase, leading to inhibition of STAT1. Trans-tympanic administration of the A_1AR agonist *R*-phenylisopropyladenosine (*R*-PIA) inhibited cisplatin-induced ototoxicity, as measured by auditory brainstem responses and scanning electron microscopy in male Wistar rats. This was associated with reduced NOX3 expression, STAT1 activation, tumor necrosis factor-α (TNF-α) levels, and apoptosis in the cochlea. *In vitro* studies in UB/OC-1 cells, an organ of Corti immortalized cell line, showed that *R*-PIA reduced cisplatin-induced phosphorylation of STAT1 Ser^{727} (but not Tyr^{701}) and STAT1 luciferase activity by suppressing the ERK1/2, p38, and JNK mitogen-activated protein kinase (MAPK) pathways. *R*-PIA also decreased the expression of STAT1 target genes, such as TNF-α, inducible nitric oxide synthase (iNOS) and cyclooxygenase-2 (COX-2) and reduced cisplatin-mediated apoptosis. These data suggest that the A_1AR provides otoprotection by suppressing NOX3 and inflammation in the cochlea and could serve as an ideal target for otoprotective drug therapy.

Key words: adenosine; adenosine receptors; cisplatin; hearing loss; inflammation; STAT1

Significance Statement

Cisplatin is a widely used chemotherapeutic agent for the treatment of solid tumors. Its use results in significant and permanent hearing loss, for which no US Food and Drug Administration-approved treatment is currently available. In this study, we targeted the cochlear adenosine A_1 receptor (A_1AR) by trans-tympanic injections of the agonist *R*-phenylisopropyladenosine (*R*-PIA) and showed that it reduced cisplatin-induced inflammation and apoptosis in the rat cochlea and preserved hearing. The mechanism of protection involves suppression of the NOX3 NADPH oxidase enzyme, a major target of cisplatin-induced reactive oxygen species (ROS) generation in the cochlea. ROS initiates an inflammatory and apoptotic cascade in the cochlea by activating STAT1 transcription factor, which is attenuated by *R*-PIA. Therefore, trans-tympanic delivery of A_1AR agonists could effectively treat cisplatin ototoxicity.

Introduction

Adenosine is a ubiquitous metabolite of ATP, which mediates its physiological actions in part by activating adenosine A_1 receptors (A_1ARs). These receptors have been extensively characterized for their role in cytoprotection. Activation of the A_1AR protects against ischemic and oxidative stress in the cardiovascular system, renal system, and CNS. Several effector systems regulated by the A_1AR, such as adenylyl cyclase, K^+ channels, and antioxidant

Received Aug. 17, 2015; revised Feb. 16, 2016; accepted Feb. 26, 2016.

Author contributions: T.K., S.J., D.M., L.P.R., and V.R. designed research; T.K., V.B., S.S., K.S., S.G., S.T., D.M., and V.R. performed research; V.R. contributed unpublished reagents/analytic tools; T.K., V.B., S.S., K.S., S.J., D.M., and V.R. analyzed data; T.K., S.S., L.P.R., and V.R. wrote the paper.

This work was supported by the National Institutes of Health (Grants R01 CA166907 and R15DC011412 to V.R. and Grant R01-DC 002396 to L.P.R.) and the American Hearing Research Foundation (S.S.). We thank Craig A. Whitworth and Anna Travelstead for scanning electron microscopy and flow cytometry, respectively, and Brandon Cox for technical assistance in developing the explants culture model in our laboratory.

*T.K. and V.B. contributed equally to this work.

The authors declare no competing financial interests.

Correspondence should be addressed to Dr. Vickram Ramkumar, Department of Pharmacology, Southern Illinois University School of Medicine, P.O. Box 19629, Springfield, IL 62794-9629. E-mail: vramkumar@siumed.edu.

DOI:10.1523/JNEUROSCI.3111-15.2016

 0270-6474/16/363962-16$15.00/0

enzymes, likely contribute to cytoprotection (Fredholm et al., 2011). A cytoprotective role of adenosine has been clearly defined in the CNS. For example, adenosine protects against transient ischemia (Daval et al., 1989; Rudolphi et al., 1992) and against audiogenic seizures (De Sarro et al., 1991). Activation of the A_1AR plays an important role in limiting seizures and the subsequent neuronal cell death resulting from them (Boison, 2006). Accordingly, a lack of A_1AR predisposes mice to seizure-induced deaths (Fedele et al., 2006; Kochanek et al., 2006). In contrast, induction of *A_1AR* expression in the rat brain by chronic caffeine ingestion renders these animals more resistant to cerebral ischemia (Rudolphi et al., 1989), whereas downregulation of these receptors exacerbated the ischemic damage (von Lubitz et al., 1994). Adenosine is also an important mediator of ischemic preconditioning, a process by which prior ischemic challenges confer resistance to subsequent ischemic damage (Schulte et al., 2004; Lankford et al., 2006).

A role of adenosine in cochlear functions was suggested from early experiments in the frog labyrinth system, a model system for studying hair cell function. These experiments indicate modulation of afferent neurotransmission in hair cells by adenosine (Bryant et al., 1987). Studies from our laboratory (Ramkumar et al., 1994) were the first to provide direct evidence of cochlear A_1AR in rat. At approximately the same time, Nario et al. (1994) demonstrated that perilymphatic perfusion of adenosine decreased endocochlear potentials in the guinea pig. We have also shown that administration of the A1AR agonist *R*-phenylisopropyladenosine (*R*-PIA) to rats via round window application increased the activities of antioxidant enzymes and reduced lipid peroxidation in the cochlea *in vivo* (Ford et al., 1997), supporting a protective role of the cochlear A_1AR. *R*-PIA was also shown to protect cochlear explants from damage induced by cisplatin (Hu et al., 1997) and against noise-induced loss of hair cells in the rat cochlea (Hight et al., 2003).

More recent studies have confirmed the protective role of adenosine and the A_1AR in cochlear protection. For example, the adenosine amine congener (ADAC) protected against noise-induced hearing loss when administered by the intraperitoneal route (Vlajkovic et al., 2010). A combination of *R*-PIA and glutathione monoethylester protects against noise-induced hearing loss in the chinchilla cochlea. Furthermore, elevation of adenosine levels by inhibition of adenosine kinase protected against age-related hearing loss (Vlajkovic et al., 2011) and ADAC protected against cisplatin ototoxicity (Gunewardene et al., 2013).

A role of inflammation in sensorineural hearing loss is supported by several observations. For example, middle ear infection (otitis media; Paparella et al., 1972) and meningitis (Merchant and Gopen, 1996) are usually associated with hearing loss in children. Noise trauma could also induce an inflammatory response in the inner ear (Fujioka et al., 2006). A recent study has shown that cisplatin-induced ROS generation is a key contributor to cochlear inflammation and apoptosis of cells in the cochlea (Kaur et al., 2011). In this study, we show that ROS activation of signal transducer and activator of transcription 1 (STAT1) contributes to cisplatin-induced inflammation and ototoxicity. Moreover, we show that the A_1AR-mediated protection involves suppression of ROS-dependent inflammatory response in the cochlea.

Materials and Methods

Drugs and reagents. Cisplatin (-)-N^6-(2-Phenylisopropyl)-adenosine (*R*-PIA), 8-Cyclopentyl-1,3-dipropylxanthine (DPCPX), diphenyleneiodonium (DPI), and TRI reagent, ERK1/2 inhibitor (PD98059) were purchased from Sigma-Aldrich. 2′,7′-dichlorodihydrofluorescein diacetate (H_2DCFDA) dye for ROS generation was from EMD Biosciences. JNK inhibitor (SP600125) was from Tocris Bioscience and p38 inhibitor (SB230580) was from Calbiochem. Various antibodies used and their dilutions were as follows: STAT1 (1:5000), inducible nitric oxide synthase (iNOS, 1:1000), cyclooxygenase-2 (COX-2, 1:1000), tumor necrosis factor-α (TNF-α, 1:500), p-STAT1 (1:1000) (both serine 727 and tyrosine 701), caspase-3 (1:1000), Bcl2 (1:1000), Phospho p38 and p38 (1:1000) (all from Cell Signaling Technology). Rabbit polyclonal myosin VIIA antibody (1:200) was from Proteus Biosciences (catalog #25-6790). Phospho ERK1/2 (1:2000) and ERK1/2 (1:4000), A_1AR (1:100), goat anti-rabbit, donkey anti-goat, and goat anti-mouse secondary antibodies were from Santa Cruz Biotechnology. Fluorescent-tagged (Dylight 488 and TRITC) secondary antibodies were from Jackson ImmunoResearch.

Animal procedures and sample collection. Male Wistar rats (200–250 g) were used for this study. Pretreatment auditory brainstem responses (ABRs) were performed immediately before trans-tympanic application of *R*-PIA or DPCPX + *R*-PIA for 1 h. Cisplatin (11 mg/kg) was administered intraperitoneally over a period of 30 min using an infusion pump in rats anesthetized with ketamine and xylazine. There was no evidence of middle ear effusion or infection in these animals. Posttreatment ABRs were then performed 72 h after cisplatin administration. Cochleae were dissected and used for total RNA and perfused with 2.5% glutaraldehyde for scanning electron microscopy (SEM) or with 4% paraformaldehyde for immunohistochemistry. All animal procedures used were approved by the Southern Illinois University Laboratory Animal Care and Use Committee.

Trans-tympanic administration of adenosine A_1 receptor agonist and antagonist. The procedure used for trans-tympanic administration of adenosine A_1 receptor agonist and antagonist was similar to that used in our laboratory in rats previously (Mukherjea et al., 2010). Rats were anesthetized with ketamine and xylazine. Fifty microliters of solution were injected into the middle ear (drugs were resuspended in 50 μl solution, pH 7.2, for the desired concentration). The rat was then left undisturbed for 15 min with the treated ear facing up. This procedure was then repeated in the other ear.

Evoked potentials. ABRs were determined as described previously (Mukherjea et al., 2008). Animals were tested with a stimulus intensity series that was initiated at 10 dB SPL and reached a maximum at 90 dB SPL, with 10 dB increments. The auditory stimuli included tone bursts at 8, 16, and 32 kHz with a 5 ms plateau and a 1 ms rise/fall time presented at a rate of 5 /s. Threshold was defined as the lowest intensity capable of evoking a reproducible, visually detectable response with two distinct waveforms (from waves 2 and 3) and minimum amplitude of 0.5 μV. These waves were chosen because they consistently showed the highest amplitudes and were more responsive to lower sound levels.

Morphological studies by SEM. Immediately after completion of posttreatment ABRs, deeply sedated rats were killed and their cochleae were harvested and processed as described previously (Mukherjea et al., 2008). Sputter-coated cochleae were then viewed and photographed with a Hitachi S-500 scanning electron microscope.

Hair cell count. Hair cell counts were performed as described previously (Mukherjea et al., 2008). Two representative areas of the basal turn, middle turn, and apex and hook portion were photographed. In each area, outer hair cells (OHCs) were counted in an area that was 10 pillar cell heads in length. The results are presented as the percentage hair cell damage per cochlear turn. At least three cochleae from different animals per treatment group were used.

Processing of cochleae for immunohistochemistry. Cochleae were perfused with 4% paraformaldehyde, decalcified in 0.1 M EDTA, pH 7.4, at room temperature for 2 weeks, paraffin embedded, and sectioned. Immunolabeling studies were performed as described previously (Mukherjea et al., 2008, 2011). Slides were then imaged using a Leica confocal microscope. Images were analyzed and quantified using the Leica confocal microscope software (LAS AF Lite). From each sample, immunofluorescence readings were captured from five different regions of the stria vascularis and spiral ligament or individual cells (for the spiral ganglion and hair cells). Ten cells were counted for each sample in the spiral ganglion and three OHCs were counted in organ of Corti. Care was taken to choose sections from approximately the same area (basal turn) of the cochlea. The readings were averaged to give the final fluorescence for

each cochlear region. Other decalcified samples were used for whole-mount preparations, which were used to show expression of A_1AR and myosin VIIA in the inner hair cells (IHCs) and OHCs.

TUNEL assay in cochlear sections. In vivo apoptosis was detected by TUNEL assay using Fluorescein FragELTM DNA fragmentation detection kit (EMD Biosciences). Briefly, cochleae were perfused with 4% paraformaldehyde, decalcified for 2 weeks, paraffin embedded, and sectioned. The cochlear sections were then deparaffinized and rehydrated, followed by permeabilization of the sections using proteinase K (1:100 dilution) (provided in the kit) for 20 min at room temperature. At the end of incubation, the slides were rinsed with 1× Tris-buffered saline (TBS). The slides were then incubated with 1× terminal deoxynucleotidyl transferase (TdT) equilibration buffer for 10–30 min. After the incubation was over, 60 μl of TdT labeling reaction mixture was applied on each section and the slides were the placed in a humidified chamber and incubated for 1–1.5 h at 37°C. Next, the slides were rinsed twice with 1× TBS. Glass coverslips were mounted using Fluorescein-FragELTM mounting medium. Excess mounting media was wiped off and the edges were sealed using nail polish. Slides were then imaged using a Leica confocal microscope.

Cell culture. Immortalized organ of Corti cells derived from the mouse, UB/OC-1 cells, were obtained from Dr. Matthew Holley (Institute of Molecular Physiology, Sheffield, UK) and cultured in RPMI 1640 supplemented with 10% Fetalclone II serum (Hyclone), penicillin/streptomycin, and normocin (Invitrogen). Cultures were grown at 33°C in an incubator with 10% CO_2.

H2DCFDA assay. ROS generation was measured with the green fluorescent dye H2DCFDA as described previously (Mukherjea et al., 2008). Briefly, UB/OC-1 cells were treated with DPCPX (3 μM) for a half hour, followed by *R*-PIA (1 μM) for another half hour. Cells were then treated with cisplatin for 15 min, followed by incubation with 5 μM H2DCFDA dye for 15 min. ROS generation was detected as green fluorescence by confocal microscopy.

Immunocytochemistry. To detect nuclear translocation of p-STAT1 after cisplatin treatment by immunofluorescence staining, UB/OC-1 cells were first plated in a 12 well plate. After the cells adhered to the plate surface, they were treated with 3 μM DPCPX for a half hour and then with *R*-PIA (1 μM) for another half hour. At the end of incubation period, cells were treated with cisplatin (2.5 μM) for 45 min. After the treatment, the cells were fixed with 4% paraformaldehyde (Sigma-Aldrich), followed by washing with 1× PBS. Coverslips were then incubated with solution A, a mixture of 5% donkey serum (Jackson ImmunoResearch) and 0.5% Triton-X (Sigma-Aldrich) in PBS for 30 min at room temperature. Primary antibody against p-STAT1 (1:300 dilution) in solution A was then added and incubated at 4°C overnight. After 3 washes with 1× PBS, the cells were incubated with Dylight 488-labeled anti-rabbit secondary antibody (1:600 dilution) in the dark for 1 h. After 3 washes with 1× PBS and 2 washes with fresh distilled water, the coverslips were mounted on glass slides using Vectashield mounting medium (Vector Laboratories) before examination under a Leica confocal microscope.

Apoptosis detection by flow cytometry. Apoptotic cells were labeled and visualized using an FITC Annexin V Apoptosis detection kit (BD PharMingen). Briefly, UB/OC-1 cells were treated with DPCPX (3 μM) for a half hour, followed by *R*-PIA (1 μM) for another half hour. Cells were then treated with cisplatin (20 μM) for another 24 h. At the end of the treatment, the cells were washed with PBS and harvested in a 0.5% trypsin/EDTA solution at 37°C, centrifuged at 220 × *g* for 5 min, and then immediately resuspended in the buffer provided in the kit. Cells (1×10^5 cells/500 μl) were then maintained in the dark for 15 min at room temperature with 5 μl of both FITC-conjugated Alexa Fluor V and propidium iodide and samples were analyzed immediately by a flow cytometry (BD FACSCalibur). The results were analyzed using the CellQuest software provided with the FACSCalibur. Early apoptotic cells are displayed in the lower right quadrant of each dot plot; necrotic or late apoptotic cells are reported in the upper right quadrant of the plot.

Flow cytometry for A_1AR expression. UB/OC-1 cells were treated with either vehicle or cisplatin (2.5 μM) for 24 h. At the end of the 24 h incubation period, the cells were resuspended in 1× PBS + 10% fetal calf serum + 1% sodium azide solution, followed by staining with the unconjugated primary antibody solution of goat polyclonal A_1AR IgG (catalog #sc-7500; Santa Cruz Biotechnology) at a 1:200 dilution in 3% BSA in 1×PBS at 4°C for 30 min. After washing the pellet twice with 1× PBS, the cells were stained with secondary antibody solution (FITC goat anti-rabbit; 1:100 in 3% BSA in 1× PBS) for 30 min in the dark at 4°C. Finally, the pellet was resuspended in 1× PBS + 3% BSA + 1% sodium azide solution and labeled cells were analyzed by flow cytometry (BD FACSCalibur). The results were analyzed using the Cell Quest software provided with the FACSCalibur.

Luciferase assay. UB/OC-1 cells were transfected with 0.8 μg of STAT1 p84/91 from Panomics and 0.2 μg of pGL3 Renilla, a kind gift from Dr. Y.Y Mo (University of Mississippi Medical Center, Jackson, MS) using SuperFect transfection reagent (Qiagen). Briefly, for each well of a 12 well plate, plasmid DNA mixed in 75 μl of serum-free media, 0.8 μg of STAT1 luciferase plasmid, and 0.2 μg of pGL3 Renilla luciferase plasmid was diluted, mixed, and incubated for 5 min. Transfection reagent (6 μl) was added to the above solution, vortexed gently, and incubated for 10 min at room temperature. The DNA transfection reagent complex was then added to the wells containing 400 μl of serum-free medium. The serum-free medium was changed with whole serum medium after 6 h and the plate was incubated for another 30 h at 33°C. Pretreatments with DPCPX (3 μM) and *R*-PIA (1 μM) were performed for 30 min, followed by treatment with cisplatin (2.5 μM) for another 8 h. Luciferase activity was assessed with the Dual-Luciferase Reporter Assay kit (Promega) according to the manufacturer's protocol. Briefly, the cells were harvested using the lysis buffer provided in the kit. Next, 25 μl of the lysate was mixed with 25 μl of luciferase assay substrate and luciferase activity was measured using a Berthold detection system luminometer. To measure the activity of the control Renilla luciferase, 25 μl of Stop & Glo substrate (Promega) was then added to the lysate mixture and luminescence was measured again. Renilla luciferase was used for normalization.

Western blot analysis. UB/OC-1 cells were homogenized in ice-cold 50 mM Tris HCl, 10 mM $MgCl_2$, and 1 mM EDTA in the presence of protease inhibitor mixture (Sigma-Aldrich) and phosphatase inhibitor 1 (Sigma-Aldrich). The whole-cell lysates were then used for Western blotting as described previously (Jajoo et al., 2009). After transfer to nitrocellulose membranes, blots were probed with different primary antibodies, followed by a horseradish peroxidase-tagged secondary antibody, and visualized by chemiluminescence detection (Pierce Biotechnology) using charged-coupled device LAS 4000 (Fujifilm). Densitometric analysis of the blots was performed with MultiGauge version 2.0 software.

RNA isolation and real time RT-PCR. RNA was isolated from UB/OC-1 cell cultures and rat cochleae by adding 1 ml of TRI reagent to 100 mg of each cochlea or 0.5 ml of TRI reagent per well of each 6 well plate and real-time RT-PCR studies were also performed as described previously (Mukherjea et al., 2008, 2011). The cycle number at which the sample reaches the threshold fluorescent intensity was termed the cycle threshold (Ct). The relative change in mRNA levels between untreated control (1) and treated sample (2) was measured using the following formula: $2^{(\text{Ct Target gene1} - \text{Ct GAPDH1}) - (\text{Ct Target gene2} - \text{Ct GAPDH2})}$ (Soong et al., 2001). Negative controls for both target gene and GAPDH were used for all reaction groups. Gene-specific primer pairs were used for the various reactions and mRNA expression levels were normalized to the levels of GAPDH. The primer sets were purchased from Sigma-Aldrich and were as follows:

Rodent-GAPDH (sense): 5′-ATGGTGAAGGTCGGTGTGAAC-3′; (antisense): 5′-TGTAGTTGAGGTCAATGAAGG-3′; rodent-NOX3 (sense): 5′-GTGAACAAGGGAAGGCTCAT-3′; (antisense): 5′-GACCCACAGAAGAACACGC-3′; rodent-STAT1 (sense): 5′-CATGGAAATCAGACAGTACCT-3′; (antisense): 5′-TCTGTACGGGATCTTCTTGGA-3′; rodent-TNF-α (sense): 5′-CAGACCCTCACACTCAGATCA-3′; (antisense): 5′-TGAAGAGAACCTGGGAGTAGA-3′; rodent-iNOS (sense):5′-CATTCTACTACTACCAGATC-3′; (antisense): 5′-ATGTGCTTGTCACCACCAG-3′; rodent-COX-2 (sense): 5′-TGATCGAAGACTACGTGCAAC-3′; (antisense): 5′-GTACTCCTGGTCTTCAATGTT-3′; rodent-A_1AR (sense): 5′-CATCCCACTGGCCATCCTTAT-3′; (antisense): 5′-AGGTATCGATCCACAGCAATG-3′.

Cochlear explant cultures. Cochleae were extracted from neonatal mice at postnatal day 3 (P3) to P5 in dissection medium containing 1× HBBS

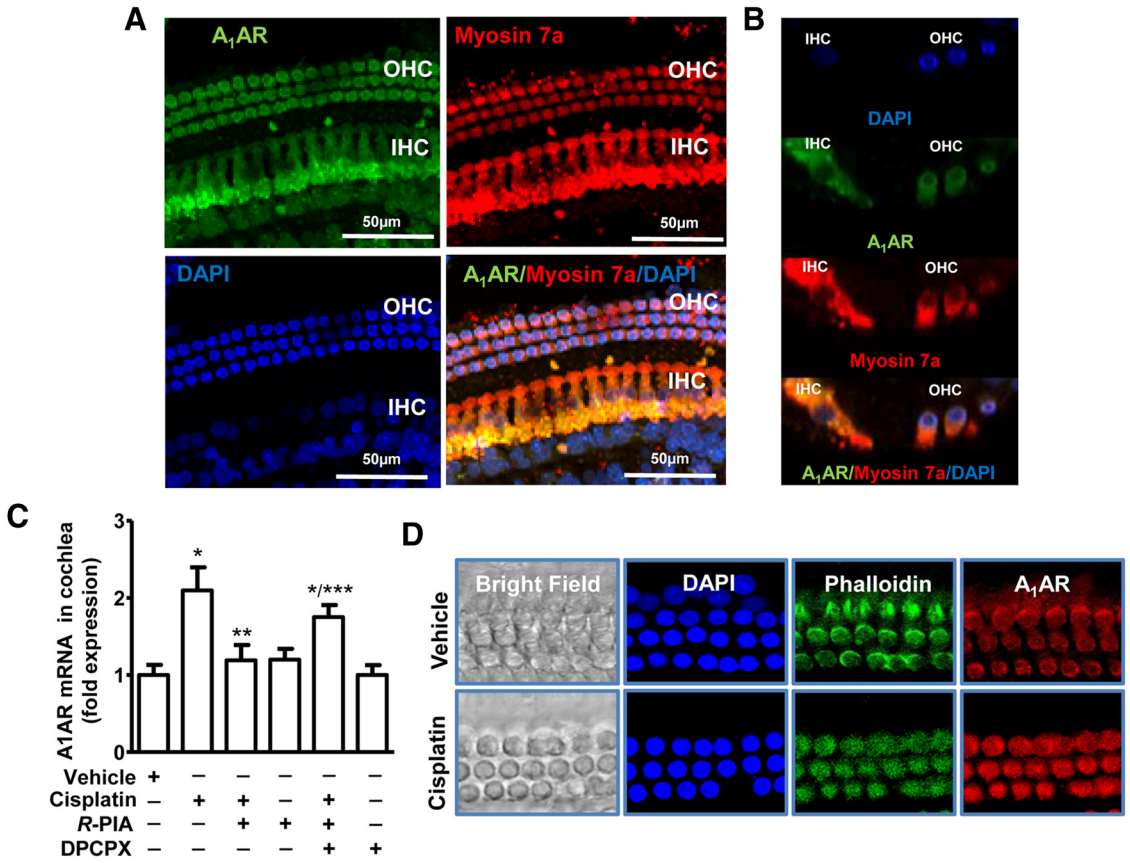

Figure 1. Presence of A_1AR in rat cochlear hair cells. ***A***, Whole-mount preparations of adult rat organ of Corti were stained with antibodies against the A_1AR, myosin VIIA, or DAPI and imaged by confocal microscopy. High levels of A_1AR immunoreactivity was observed in IHCs, with lower levels in OHCs. Similar patterns of myosin VIIA immunolabeling was detected, with a significant degree of colocalization in IHCs. Orthogonal sections of these images are shown in ***B*** and indicate localization of A_1AR to IHCs and OHCs with a significant degree of colocalization. ***C***, Rat were treated with cisplatin (11 mg/kg, i.p.), killed 3 d later, and their cochleae were dissected out and processed for RNA and for expression of A_1AR by real-time PCR. Cisplatin produced a significant increase in A_1AR expression, which was blocked by *R*-PIA. Pretreatment with DPCPX before *R*-PIA reversed the inhibition of A_1AR induction by cisplatin. *Statistically significant difference from vehicle-treated group; **statistically significant difference from cisplatin-treated group; ***statistically significant difference from *R*-PIA-treated group ($n = 5, p < 0.05$). ***D***, Rats were treated with vehicle or cisplatin (11 mg/kg, i.p.), killed 3 d later, and their cochleae were dissected out, decalcified over a 3 week period, and used for whole-mount preparations. These preparations were stained and imaged by confocal microscopy. Images of OHCs show increased levels of A_1AR immunoreactivity with little change in myosin VIIA.

and 25 mM HEPES, pH 7.5. They were then transferred to a 35 mm Petri dish containing explant culture media (DMEM with glucose and glutamine + 1% FCS + ampicillin and ciprofloxacin) and the organs of Corti (explants) were isolated. The explants were cultured at 37°C in 5% CO_2 for 1 d before drug treatment.

Morphological studies by cochlear whole-mount preparation. Isolated adult rat cochleae were perfused with 4% paraformaldehyde and kept overnight at 4°C in the same solution for fixation. Then, cochleae were decalcified in 0.1 M EDTA, pH 7.4, with stirring at room temperature for 2 weeks. After decalcification, the cochleae were microdissected into basal, middle, and apical turns for whole-mount preparation.

Statistical analysis. Data are presented as mean ± SEM. Statistical significance differences among groups were performed by either Student's *t* test or ANOVA followed by Tukey's *post hoc* test wherever appropriate.

Results

A_1ARs are expressed on cochlear OHCs

We have shown previously that the rat cochlea expresses A_1ARs, the activation of which led to inhibition of adenylyl cyclase activity (Ramkumar et al., 1994), stimulation of antioxidant enzymes, and a reduction in lipid peroxidation (Ford et al., 1997a). Additional studies have also shown that the chemotherapeutic agent cisplatin induces the expression of the cochlear A_1AR, which likely represents a compensatory mechanism by the cochlea to counter the toxic effects of increased ROS generation by cisplatin (Ford et al., 1997b). Activation of A_1AR was also shown to confer protection of OHCs against cisplatin-induced damage and death and hearing loss (Whitworth et al., 2004; Gunewardene et al., 2013). However, it has been suggested that A_1ARs are not localized to OHCs, but rather are found on IHCs, Deiter's cells, and spiral ganglion (SG) neurons (Vlajkovic et al., 2009). In whole-mount preparations obtained from adult rats, we show A_1AR immunoreactivity on both OHCs and IHCs (Fig. 1*A*), where they colocalize with myosin VIIA, a marker of hair cells. However, A_1AR immunolabeling was certainly more intense in IHCs, as reported earlier (Vlajkovic et al., 2007, 2009). Quantification of immunofluorescence shows A_1AR staining in IHCs was 115 ± 5% of that observed in OHCs (mean ± SEM, $n = 4$). Orthogonal sections (Fig. 1*B*) clearly show staining for the A_1AR in OHCs from rat cochlea. Cisplatin increased the expression of A_1AR in the cochlea, as indicated by qPCR studies ($n = 5$, Fig. 1*C*). Interestingly, this effect was attenuated by the A_1AR agonist *R*-PIA, suggesting that activation of the A_1AR negatively influences its induction by cisplatin. Similarly, we observed an increase in A_1AR immunolabeling of 52 ± 7% ($n = 5$, $p < 0.05$) in the OHCs 3 d after cisplatin treatment

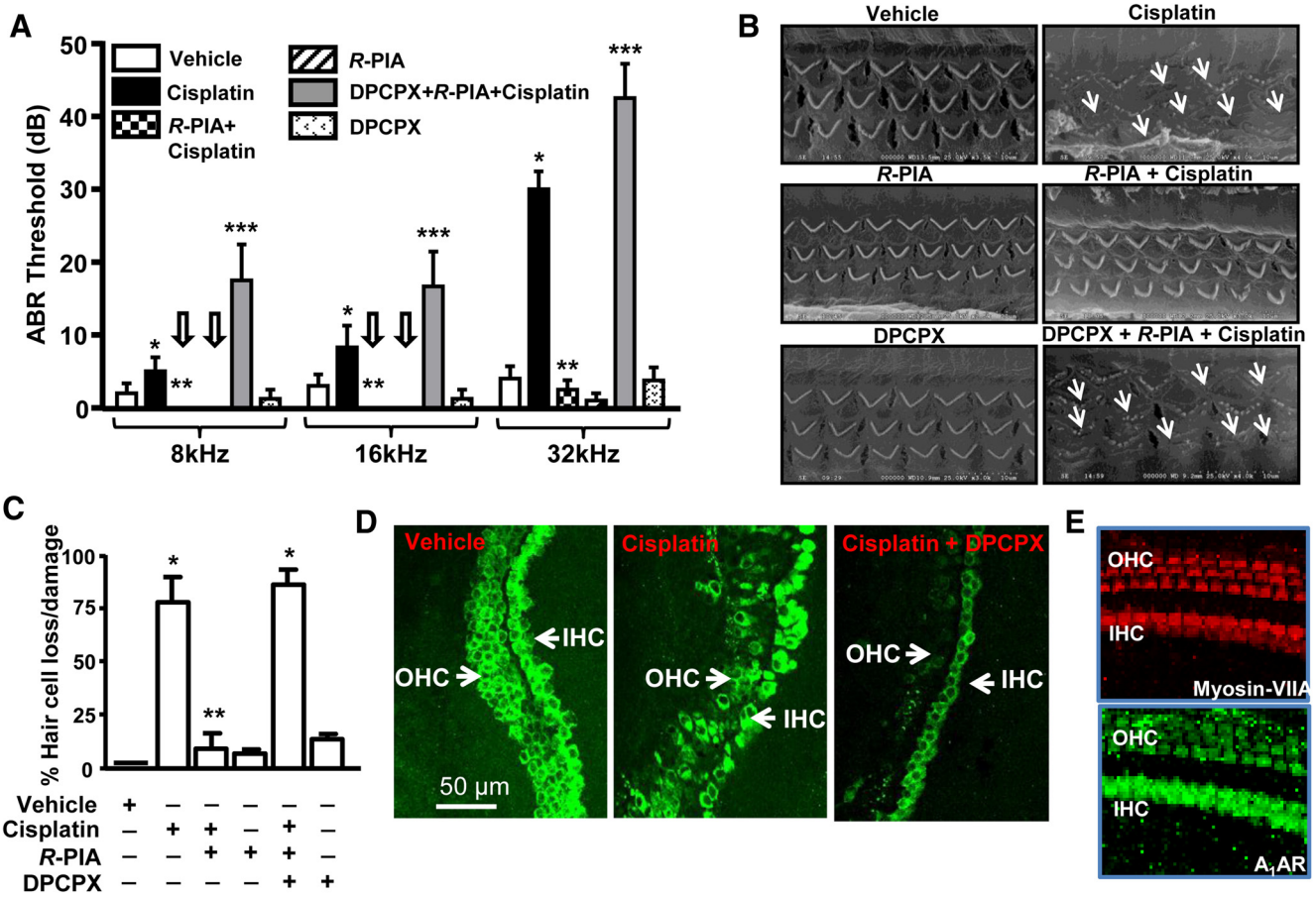

Figure 2. Activation of the A_1AR leads to inhibition of cisplatin-induced hearing loss in rats. ***A***, ABR thresholds were recorded in Wistar rats treated with cisplatin (11 mg/kg, i.p.) after trans-tympanic administration of *R*-PIA (1 μM) or DPCPX (3 μM) + *R*-PIA. Posttreatment ABRs, determined 3 d later, showed significant elevations in ABR thresholds, which were attenuated by *R*-PIA. The protective effect of *R*-PIA was reversed by DPCPX, which significantly enhanced the ABR shifts produced by cisplatin at all frequencies tested. Arrows indicate 0 ABR threshold shift. ***B***, SEM studies performed on the cochleae show significant damage to OHCs (white arrows) by cisplatin, which was protected by the A_1AR agonist *R*-PIA and exacerbated by DPCPX. ***C***, Quantitative analysis of the SEM images. ***D***, DPCPX exacerbates cisplatin-induced loss of OHCs without affecting IHCs. Cochlear explants from P5 mice were treated with vehicle, cisplatin, or cisplatin + DPCPX (1 μM) for 48 h, stained for myosin VIIA, and imaged by confocal microscopy. ***E***, Expression of A_1AR in adult mouse organ of Corti. In these images, red represents myosin-VIIA and green represents A_1AR. Data in ***A*** and ***C*** are presented as mean ± SEM of five rats. Images shown in ***B*** and ***D*** are representatives of five similar images from different rats. *Statistically significant difference from vehicle-treated group; **statistically significant difference from cisplatin-treated group; ***statistically significant difference from cisplatin-treated group ($p < 0.05$, $n = 5$).

(Fig. 1*D*), but a significant decrease in myosin VIIA immunoreactivity of 25 ± 4% ($n = 5$, $p < 0.05$).

Activation of A_1AR prevented cisplatin-induced hearing loss and damage to OHCs

Previous studies have indicated that round window application of *R*-PIA reduced cisplatin-induced hearing loss and hair cell damage (Whitworth et al., 2004). In this study, we showed a similar effect of *R*-PIA when administered by the trans-tympanic route. Male Wistar rats were treated with vehicle or *R*-PIA (50 μl of 0.1 mM solution), followed by intraperitoneal administration of cisplatin (11 mg/kg) 30 min later. ABRs were assessed immediately before (pretreatment ABRs) and 3 d after cisplatin administration (posttreatment ABRs). The administration of vehicle produced minimal change in ABR thresholds from pretreatment values. Cisplatin elevated thresholds averaged 5 ± 2, 8 ± 3, and 30 ± 2 dB at frequencies of 8, 16, and 32 kHz, respectively (Fig. 2*A*). However, trans-tympanic *R*-PIA significantly attenuated cisplatin-induced changes in ABR thresholds at 8, 16, and 32 kHz ($p < 0.05$, $n = 5$). The ABR thresholds shifts in the *R*-PIA + cisplatin-treated animals were 0, 0, and 3 ± 1 dB for 8, 16, and 32 kHz, respectively, demonstrating a pronounced inhibitory effect on hearing loss assessed at different frequencies by *R*-PIA, especially at the highest frequency. Co-administration of A_1AR antagonist, DPCPX (50 μl of 0.1 mM solution), completely reversed the protective effect of *R*-PIA (Fig. 2*A*). SEM images of the organ of Corti obtained from the animals treated above showed extensive loss of OHCs in the basal turn of the cochleae obtained from animals treated with cisplatin (Fig. 2*B*). In addition, the remaining OHCs in the basal turn showed significant disruption in stereociliary bundles. The extent of the loss or damage of OHCs in the basal turn averaged 77 ± 11% (average of 4 cochleae) compared with vehicle-treated animals (Fig. 2*C*). In contrast, the organ of Corti obtained from animals pretreated with *R*-PIA before cisplatin showed significantly reduced loss or damage of OHCs in the basal turn (9 ± 7% loss of OHC). Disruption of stereociliary bundles was considerably reduced. Cochleae obtained from animals treated with *R*-PIA alone showed 7 ± 2% damage in OHC morphology that was not significantly different from vehicle-treated and *R*-PIA + cisplatin-treated rats, which could reflect damage inherent to the procedure used for sample preparation. Pretreatment with a combination of DPCPX and *R*-PIA before cisplatin resulted in greater loss of OHCs (86 ± 7%) compared with the vehicle- and cisplatin-alone-treated groups (Fig. 2*C*),

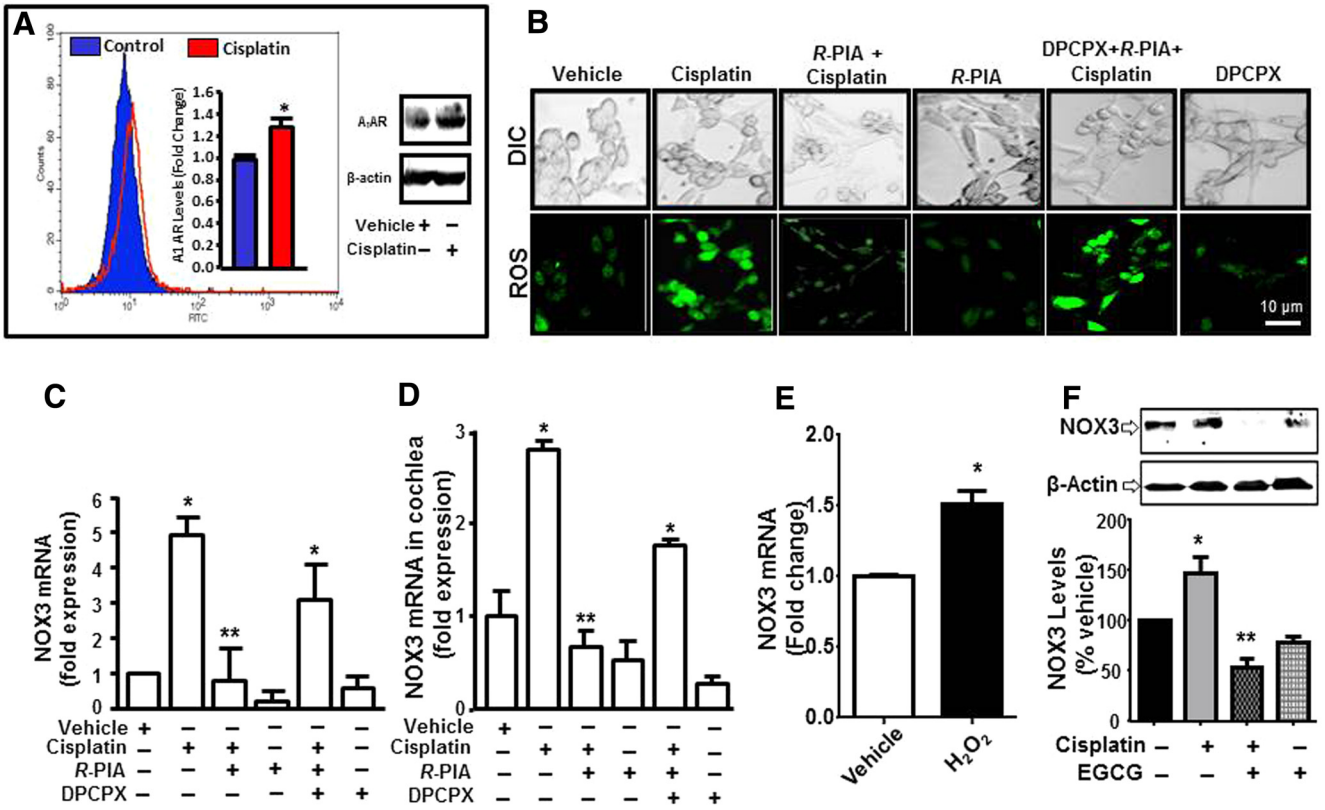

Figure 3. *R*-PIA inhibits cisplatin-induced ROS generation via NOX3. ***A***, UB/OC-1 cells express A_1AR receptors that were significantly upregulated by cisplatin. UB/OC-1 cells were exposed to vehicle or cisplatin (2.5 μM) for 24 h and processed for flow cytometry using A_1AR antibody and for Western blotting. Cisplatin significantly increased the mean fluorescence exhibited by these cells (1.39 ± 0.04 fold) and this was confirmed by Western blot data showing increased in A_1AR protein levels by $27 \pm 4\%$ and mRNA by $40 \pm 4\%$. ***B***, ROS generation was measured in UB/OC-1 cells treated with either *R*-PIA or DPCPX + *R*-PIA for 0.5 h, followed by treatment with cisplatin (2.5 μM) for 15 min. Cells were then incubated with 5 μM H_2DCFDA dye for 15 min and ROS generation (green fluorescence) was visualized by confocal microscopy. DIC, Differential interference contrast. Cisplatin increased NOX3 mRNA in the UB/OC-1 cells (***C***) and rat cochlea (***D***), as determined by quantitative real-time PCR. This response was mimicked by H_2O_2 (100 μM) treatment for 24 h (***E***). ***F***, Western blots for NOX3 after treatment with cisplatin and/or EGCG (100 μM) in UB/OC-1 cells for 24 h. Data are presented as mean $\pm$ SEM of at least four independent experiments. *Statistically significant difference from vehicle-treated group; **statistically significant difference from cisplatin-treated group ($p < 0.05$).

suggesting a partial protective action of the cochlear A_1AR activation by endogenous adenosine in the cisplatin-treated rats. These findings confirm the utility of trans-tympanic administration of *R*-PIA against cisplatin-induced hearing loss. Because the OHCs express A_1ARs, it is it is likely that activation of these receptors provided the protection afforded by the agonist. However, it is also possible that protection of the OHCs is mediated indirectly by reductions in cisplatin-induced damage to other regions of the cochlea, such as IHCs, stria vascularis (SVA), SG, or spiral ligament (SL). In addition, a previous study has shown direct inhibition by AR drugs of TRPV1 channels (Puntambekar et al., 2004), which are also expressed on OHCs (Mukherjea et al., 2008). Inhibition of these channels confers protection against cisplatin-induced hearing loss (Mukherjea et al., 2008).

In most studies, IHCs appear to be resistant to cisplatin-induced damage. We reasoned that the high expression of the A_1AR in these cells could contribute to this resistance. To examine the role of the A_1AR present on IHCs, we used organ of Corti explants from P5 mice. Explants were allowed to recover for 24 h in culture after dissection and were then incubated with vehicle, cisplatin (20 μM), DPCPX (3 μM), or DPCPX + cisplatin for 48 h. Cisplatin produced a significant loss of OHCs, with some disruption of IHCs. Blockade of the A_1AR with DPCPX potentiated the loss of OHCs, but did not significantly affect IHCs (Fig. 2*D*). Counting the OHCs per field indicated ~66% loss of myosin VIIA-stained cells in the cisplatin-treated explants, but ~88% loss of cells in the DPCPX + cisplatin-treated explants. These data suggest that activation of the A_1ARs expressed on IHCs do not confer resistance of these cells to cisplatin. Additional immunohistochemical studies indicate that the mouse cochlea expresses A_1AR, with higher levels in the IHCs than OHCs (Fig. 2*E*). Similar expression of the A_1AR was observed from the base to the apex of the cochlea (data not shown).

A_1AR activation reduces ROS generation via NOX3

Cisplatin ototoxicity is mediated in part by ROS produced via NOX3 (Bánfi et al., 2004; Mukherjea et al., 2008). ROS regulates STAT1 phosphorylation in pancreatic cancer cells by maintaining Janus kinase 2 (JAK2) in a constitutively active state (Simon et al., 1998). In addition, we have also shown that ROS activate STAT1 via the ERK1/2 pathway (Kaur et al., 2011). Therefore, we investigated whether *R*-PIA inhibits ROS generation via NOX3. These experiments were performed in UB/OC-1 cells, a cell line derived from the mouse embryonic cochlear hair cells that express hair cell markers such as Brn 3.1, myosin VIIA, and α 9 nicotinic receptor (Rivolta et al., 1998). These cells also express the A_1AR, as depicted by flow cytometry and Western blotting (Fig. 3*A*). Exposure of these cells to cisplatin for 24 h increased the levels of the A_1AR protein (Fig. 3*A*) and mRNA (by $40 \pm 4\%$). These responses are similar to those observed in the cochlea of cisplatin-treated rats (Fig. 1*D*). ROS generation was measured by live confocal imaging using H_2DCFDA dye. Cisplatin increased

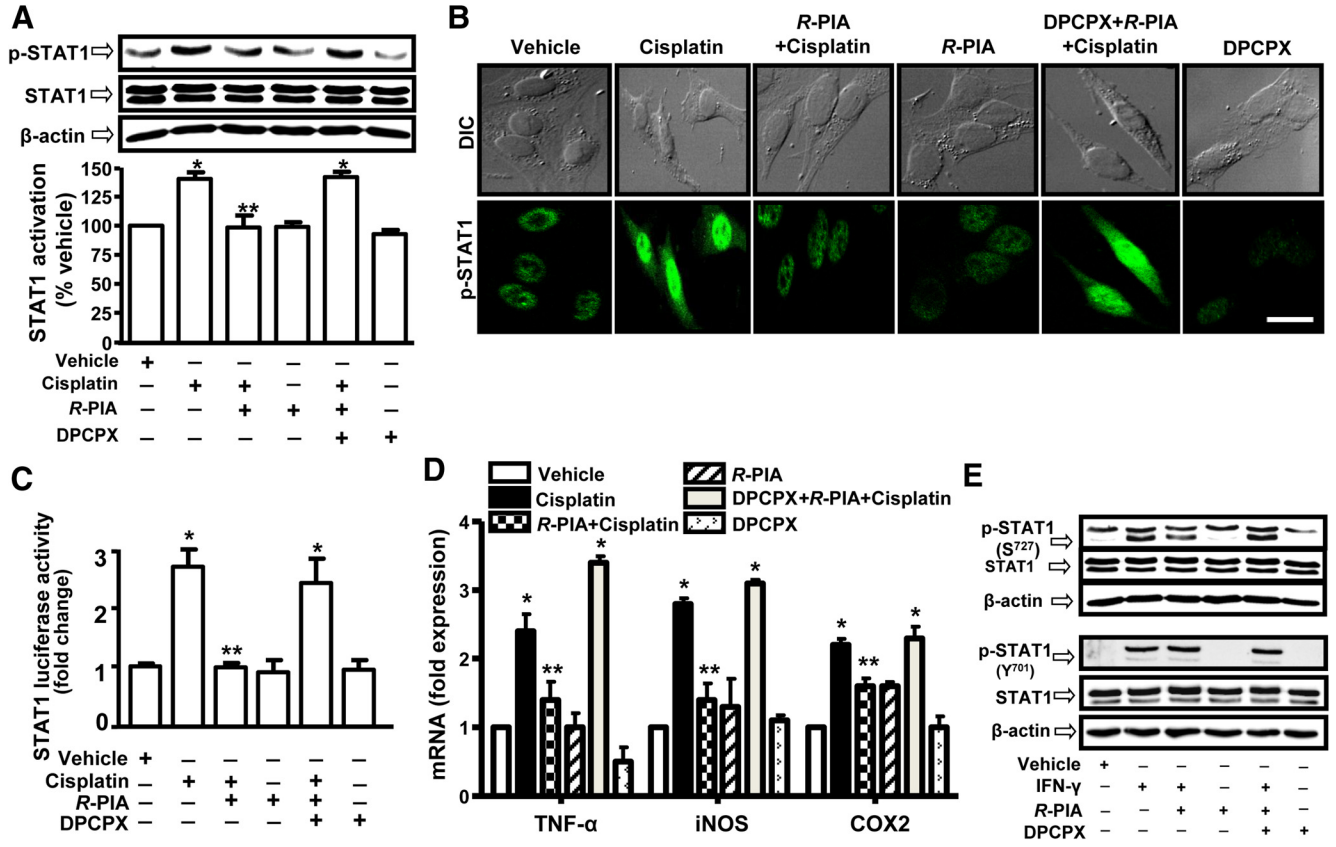

Figure 4. Cisplatin activation of STAT1 is attenuated by *R*-PIA in UB/OC-1 cells. ***A***, UB/OC-1 cells were treated with *R*-PIA for 0.5 h before cisplatin treatment for 45 min. Cell lysates were prepared and used in Western blot studies for Ser^{727} p-STAT1. ***B***, UB/OC-1 cells were pretreated with *R*-PIA or DPCPX + *R*-PIA for 0.5 h, followed by cisplatin treatment for 45 min. Cells were then fixed with 4% paraformaldehyde and stained with p-STAT1 antibody, followed by a fluorescein-tagged secondary antibody (green). Cisplatin increased p-STAT1 immunoreactivity in the UB/OC-1 cells, which coincided significantly with nuclei as seen in fluorescent images. Nuclear translocation of p-STAT1 was not observed in cells pretreated with vehicle, *R*-PIA, and DPCPX treatment alone. This is a representative of three experiments showing similar results. ***C***, UB/OC-1 cells were transfected with a plasmid vector encoding STAT1 luciferase, along with a Renilla luciferase. After 36 h of transfection, the cells were treated with *R*-PIA and DPCPX, followed by treatment with vehicle or cisplatin (2.5 μM) for 8 h. Lysates were prepared and used for determination of luciferase activity. Cotransfection of a plasmid expressing renilla luciferase allowed for normalization of luciferase activity in each well. ***D***, UB/OC-1 cells were treated with *R*-PIA for 0.5 h, followed by cisplatin (2.5 μM) for 24 h. RNA was isolated using TRIzol reagent and mRNA levels of TNF- α, iNOS, and COX-2 were determined by real-time RT-PCR. GAPDH was used as a housekeeping gene and for normalization. ***E***, *R*-PIA reduced IFN-γ mediated STAT1 activity on Ser^{727}, but not on the Tyr^{701}, phosphorylation site. Cells were exposed to *R*-PIA (1 μM) for 0.5 h, followed by treatment with IFN-γ (250 units/ml) for 1 h. Cells lysates were subjected to immunoblotting for Ser^{727} and Tyr^{701} p-STAT1. Data are presented as mean ± SEM of three independent experiments. *Statistically significant difference from vehicle-treated group; **statistically significant difference from cisplatin-treated group ($p < 0.05$, $n = 3$).

the ROS levels in the cells, as indicated by enhanced green fluorescence compared with vehicle-treated cells (Fig. 3*A*). The ROS generation by cisplatin was inhibited by pretreatment with *R*-PIA (Fig. 3*B*). *R*-PIA also attenuated NOX3 expression induced by cisplatin both in UB/OC-1 cells (Fig. 3*C*) and in the rat cochlea (Fig. 3*D*), suggesting that the A_1AR can regulate ROS generation by controlling both the activity and expression of the *NOX3* gene. Accordingly, by acting on the A_1AR, adenosine could serve as an endogenous inhibitor of NOX3 activity and expression. Interestingly, ROS positively regulates the expression of A_1AR (Nie et al., 1998). To confirm that ROS could induce NOX3 expression, we exposed UB/OC-1 cells to H_2O_2 and measured the expression of NOX3 by real-time PCR. We observed a 1.5 ± 0.1-fold increase in NOX3 when UB/OC-1 cells were exposed to 100 μM H_2O_2 for 24 h (Fig. 3*E*). Furthermore, to determine a possible mechanism of induction of NOX3, we inhibited STAT1 using EGCG (100 μM), a known inhibitor of this transcription factor. Data presented in Figure 3*F* show that EGCG inhibited the induction of NOX3 by cisplatin. These data suggest a reciprocal interaction between NOX3 and STAT1 in the cochlea.

A_1AR inhibits cisplatin-induced activation of STAT1 in UB/OC-1 cells and rat cochlea

Several studies have implicated the STAT1 transcription factor in mediating an inflammatory process in the inner ear resulting in hearing loss (Schmitt et al., 2009; Mukherjea et al., 2011; Kaur et al., 2011). We have also shown previously that cisplatin-induced STAT1 activation is mediated via ROS generation (Mukherjea et al., 2011). Because activation of A_1AR inhibits ROS generation, we investigated whether it also inhibits cisplatin-induced STAT1 activation. For these experiments, UB/OC-1 cells were pretreated with *R*-PIA (1 μM), followed by cisplatin (2.5 μM), for 45 min. The levels of Ser^{727}-phosphorylated STAT1 (Ser^{727} p-STAT1) were increased by ~40% compared with vehicle-treated cells. *R*-PIA significantly reduced the cisplatin-induced Ser^{727} p-STAT1 levels without altering the levels of total STAT1. Co-administration of DPCPX (3 μM) with *R*-PIA (1 μM) led to complete reversal of *R*-PIA-mediated inhibition of STAT1 activation produced by cisplatin (Fig. 4*A*). However, co-administration of ZM241385 (3 μM), an A_{2A}AR receptor antagonist, or MRS1523 (3 μM), an A_3AR antagonist, along with *R*-PIA did not inhibit the effect of *R*-PIA (data not shown). To-

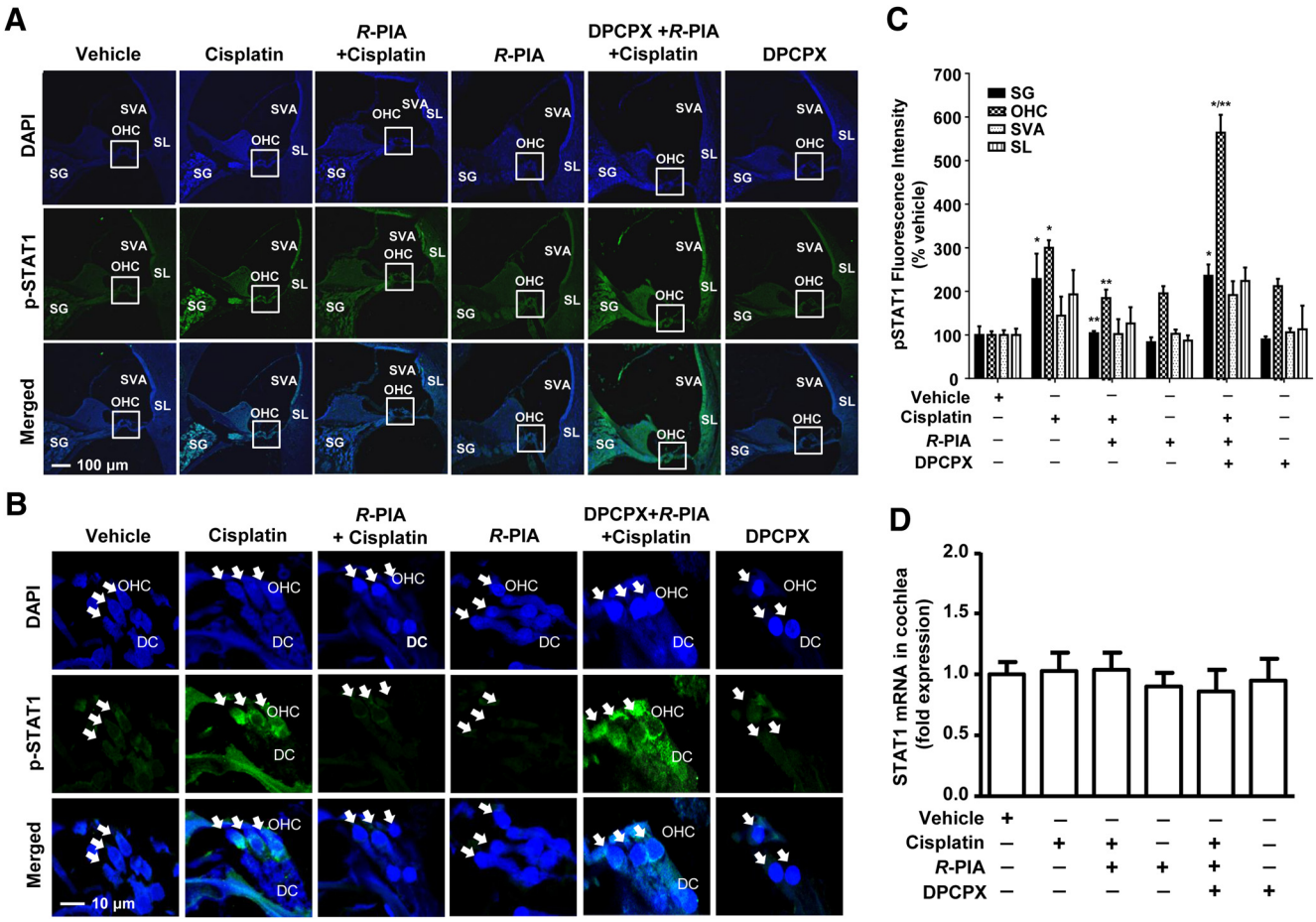

Figure 5. Cisplatin-induced activation of STAT1 is attenuated by *R*-PIA in the rat cochlea. ***A***, Immunolabeling studies were performed on the cochlear sections isolated from the rats treated with vehicle or cisplatin (11 mg/kg/i.p.) for 72 h after trans-tympanic administration of *R*-PIA (1 μM). Ser^{727} p-STAT1 immunolabeling is indicated by green fluorescence while cell nuclei are defined by DAPI staining. Statistically significant increases in immunofluorescence are observed in the OHCs (OHC) and spiral ganglion (SG) cells. Scale bar shown in the lower right panel is 100 μm. ***B***, Magnified view of the OHC from the square boxes in (***A***). Arrows indicate the three rows of OHCs. DC represents Deiter's cells. Scale bar shown in the lower right panel is 10 μm. ***C***, Quantification of p-STAT1 immunofluorescence from (***A***, ***B***). ***D***, Total STAT1 mRNA, determined by real time PCR, was not changed with any of the treatment groups in cochleae obtained from rats. Data are presented as mean ± SEM ($n = 5$). *Statistically significant difference from vehicle-treated group; **statistically significant difference from cisplatin-treated group ($p < 0.05$).

gether, these data suggest that inhibition of STAT1 by *R*-PIA is mediated specifically by the A_1AR subtype. We did not examine Tyr^{701} p-STAT1 because cisplatin was unable to induce phosphorylation of this site (Kaur et al., 2011).

Cisplatin increased nuclear translocation of p-STAT1 within 45 min, as indicated by increased nuclear immunolabeling, compared with vehicle-treated cells. Nuclear Ser^{727} p-STAT1 labeling (green color) was more intense in the cisplatin-treated cells compared with *R*-PIA alone or *R*-PIA + cisplatin-treated cells (Fig. 4*B*). The effect of *R*-PIA was blocked by DPCPX, implicating the A_1AR in this process. Cisplatin also increased STAT1 luciferase activity by 2.7 ± 0.3 fold, which was attenuated by *R*-PIA (1.0 ± 0.1-fold; Fig. 4*C*). Co-administration of DPCPX reversed the effect of *R*-PIA, as evidenced by increased STAT1 luciferase activity of 2.4 ± 0.4 fold (Fig. 4*C*). *R*-PIA also attenuated the expression of STAT1-regulated genes, such as *TNF-α*, *iNOS*, and *COX-2* (Fig. 4*D*). Cisplatin significantly increased the mRNA levels of *TNF-α*, *iNOS*, and *COX-2* by 2.4 ± 0.2, 2.8 ± 0.1, and 2.2 ± 0.1 fold, respectively, whereas pretreatment with *R*-PIA attenuated the respective increases to 1.4 ± 0.3, 1.4 ± 0.2, and 1.6 ± 0.1 fold (statistically significant inhibition for all groups, $p < 0.05$). DPCPX not only blocked the effect of *R*-PIA, but also enhanced the expression of *TNF-α*, *iNOS*, and *COX-2* by 3.4 ± 0.1, 3.1 ± 0.1, and 2.3 ± 0.2, respectively. The effect of DPCPX on cisplatin-induced *TNF-α* expression was statistically significantly different from that of cisplatin alone ($p < 0.05$), suggesting tonic suppression of the expression of this cytokine by endogenous adenosine via the A_1AR (Fig. 4*D*). We investigated whether *R*-PIA would also affect the response of interferon-γ (IFN-γ), a known activator of STAT1. Treatment of UB/OC-1 cells with IFN-γ (250 units/ml) increased phosphorylation of STAT1 at both Ser^{727} and Tyr^{701} by 3- and 2-fold, respectively, compared with vehicle-treated cells. In cells pretreated with *R*-PIA (1 μM), the IFN-γ phosphorylation of Ser^{727} STAT1 was reduced to ~1.5 fold, whereas the increased Tyr^{701} phosphorylation was unaffected (Fig. 4*E*). These data suggest that activation of A_1AR specifically inhibits the Ser^{727}, but not the Tyr^{701}, phosphorylation of STAT1, which could contribute to the inhibition of expression of STAT1 responsive genes. Accordingly, the ototoxicity produced by cisplatin and attenuated by A_1AR is attributable, at least in part, to phosphorylation of STAT1 at Ser^{727}.

Previous studies from our laboratory showed that cisplatin increased Ser^{727} p-STAT1 immunolabeling in the rat cochlea. Increased immunolabeling was observed in the OHCs, SG, and SVA (Kaur et al., 2011). We next determined whether trans-tympanic administration of *R*-PIA in rats could inhibit Ser^{727} p-STAT1 immunolabeling in the rat cochlea. Immunolabeling for Ser^{727} p-STAT1 showed low baseline Ser^{727} p-STAT1 immu-

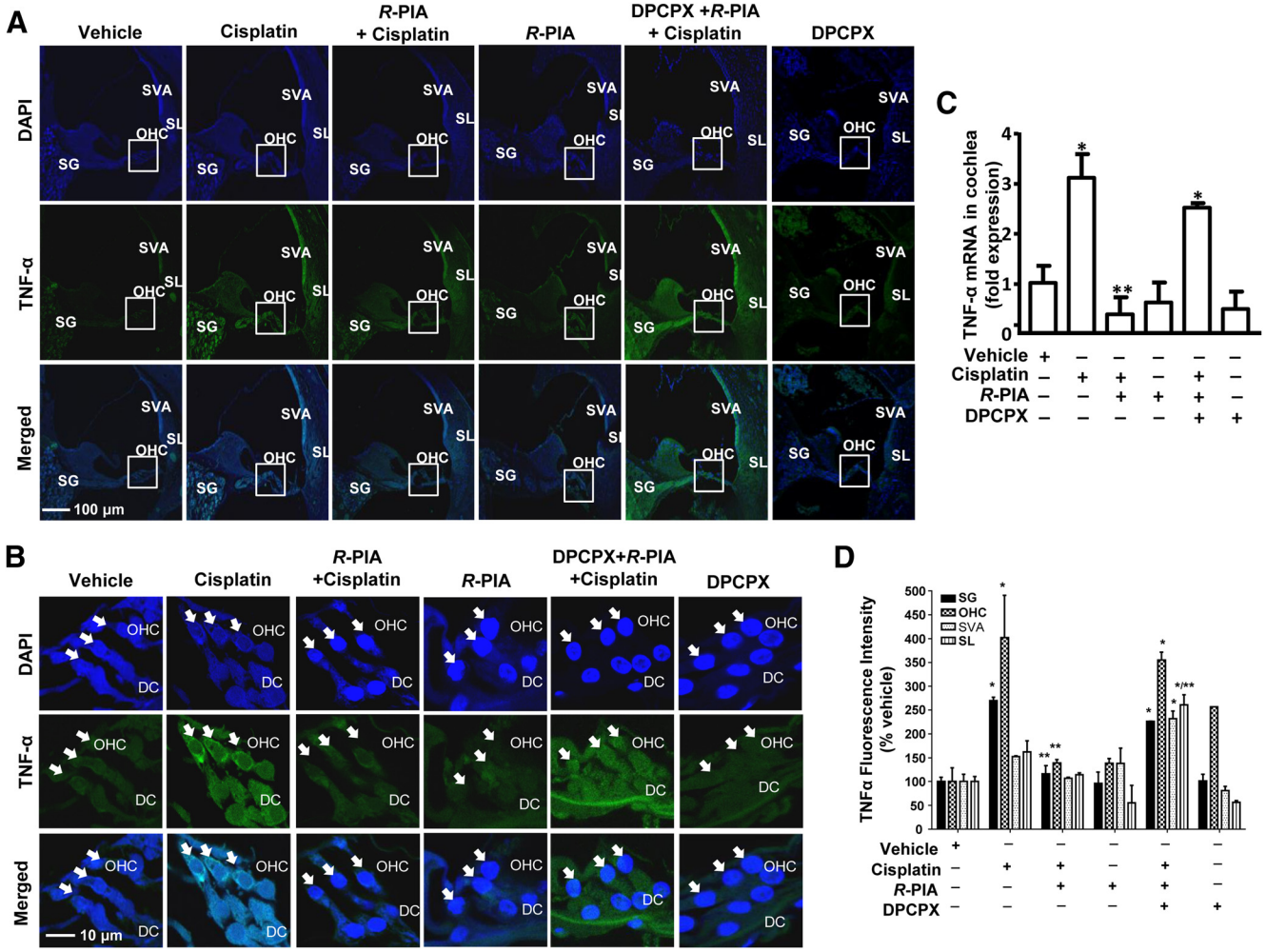

Figure 6. Adenosine A_1 receptor activation attenuates cisplatin-induced inflammation in rat cochlea. ***A***, Rats were treated with *R*-PIA or DPCPX + *R*-PIA by trans-tympanic injections, followed by vehicle or cisplatin (11 mg/kg, i.p.). Rats were killed 3 d after the administration of vehicle or cisplatin. The cochleae were excised and processed for immunohistochemistry. Mid-modiolar sections of the cochlea were labeled with TNF-α antibodies, followed by fluorescein (green)-labeled secondary antibodies and DAPI staining to label the nucleus. Cisplatin increased TNF-α immunoreactivity in cochleae treated with cisplatin. However, the increases in immunolabeling were attenuated in cochlea pretreated with *R*-PIA. Scale bars (right bottom), 100 μm. ***B***, Magnified view of the OHCs presented in ***A***. Arrows indicate three rows of OHCs. DC, Deiter's cells. Increased TNF-α immunoreactivity was observed in both OHCs and Deiter's cells. Scale bar, 10 μm. ***C***, TNF-α mRNA levels in the rat cochlea were determined by real-time PCR. Cisplatin induced increase in the mRNA levels were reduced by *R*-PIA pretreatment. Trans-tympanic administration of DPCPX, an A_1AR antagonist, reversed the effects of *R*-PIA. ***D***, Quantification of TNF-α immunoreactivity in different regions of the organ of Corti after different treatments. Data are presented as mean ± SEM. *Statistically significant difference from vehicle-treated group; **statistically significant difference from vehicle + cisplatin-treated group ($p < 0.05$, $n = 5$).

noreactivity in the cochleae from rats administered vehicle, *R*-PIA, and DPCPX alone. Cisplatin increased Ser^{727} p-STAT1 immunoreactivity in the cochleae, which was reduced by pretreatment with *R*-PIA (Fig. 5*A*). Increases in Ser^{727} p-STAT1 immunoreactivity induced by cisplatin were observed in the OHCs and SG cells, with no significant changes observed in SVA and SL cells (Fig. 5*B*). These increases were attenuated by *R*-PIA. Co-administration of DPCPX and *R*-PIA before cisplatin not only attenuated the effect of *R*-PIA, but further increased Ser^{727} p-STAT1 immunolabeling in the OHCs, but not in other regions (Fig. 5*B*). Higher-magnification images indicate increased labeling of the OHC after cisplatin or cisplatin + DPCPX treatments. Staining was also observed in regions below the OHCs, possibly reflecting labeling of Deiter's cells (Fig. 5*C*). Immunolabeling was also prominent in the basilar membrane. The levels of STAT1 mRNA remained unchanged after cisplatin treatment (Fig. 5*D*), suggesting that cisplatin activated, but did not induce, the expression of total STAT1 over this time period.

Activation of A_1AR reduces cisplatin-induced inflammation

Adenosine regulates a variety of pathophysiological processes involving neuronal damage or death (Ribeiro et al., 2002) and inflammation (Cronstein, 1994). In recent studies, the activation of ARs on immune cells suppressed the production of proinflammatory mediators, including TNF-α (Bouma et al., 1994; Haskó et al., 1996; Sajjadi et al., 1996). In addition, Tsutsui et al. (2004) demonstrated that spinal cords from A_1AR knock-out mice had increased proinflammatory gene expression during experimental allergic encephalomyelitis. Macrophages derived from A_1AR knock-out animals exhibited increased expression of the proinflammatory genes, such as interleukin-1β (IL-1β) and iNOS, upon immune activation compared with wild-type control mice. In a previous study, we showed that STAT1-induced inflammation is an important contributor to cisplatin ototoxicity (Kaur et al., 2011). Because *R*-PIA attenuated cisplatin-induced activation of STAT1 (Figs. 4, 5), these findings suggest that *R*-PIA-mediated otoprotection could similarly involve inhibition of STAT1-

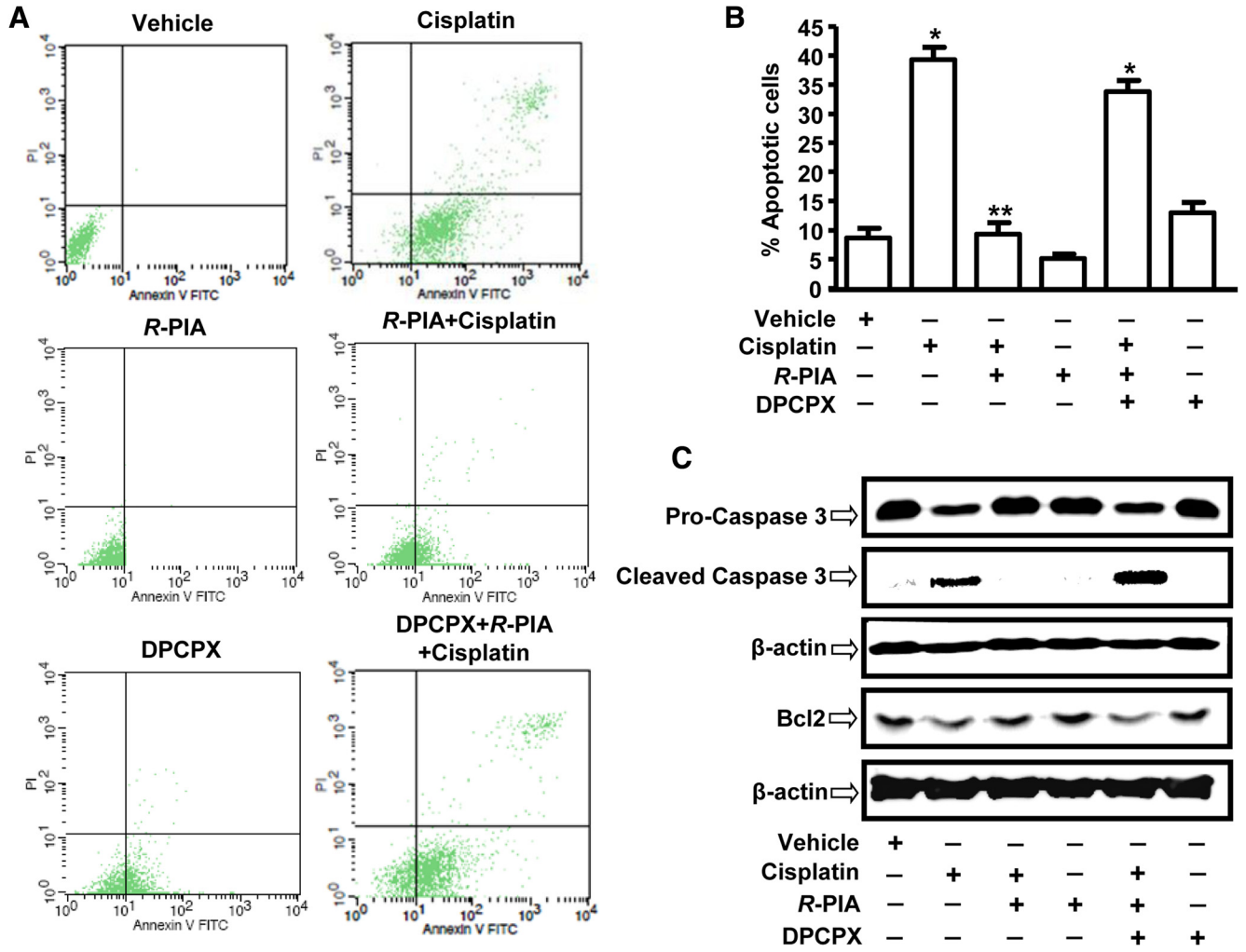

Figure 7. *R*-PIA reduced cisplatin-mediated apoptosis of UB/OC-1 cells. ***A***, UB/OC-1 cells were treated with *R*-PIA for 0.5 h, followed by cisplatin (20 μM) for an additional 24 h. Apoptosis was determined by measuring the percentage of Annexin-positive and Annexin plus propidium iodide-positive cells (lower right and upper right quadrant, respectively) by flow cytometry. ***B***, Percentage of apoptotic cells for each treatment as determined in ***A*** and plotted as the mean ± SEM ($n = 3$). *Statistically significant difference from vehicle-treated group; **statistically significant difference from vehicle + cisplatin-treated group ($p < 0.05$). ***C***, UB/OC-1 cells were treated with *R*-PIA for 0.5 h, followed by cisplatin (20 μM) for an additional 24 h. Cells lysates were used to determine the levels of cleaved caspase 3, Bcl2, and β-actin (for normalization). Cisplatin induced the cleavage of procaspase-3, which was attenuated by *R*-PIA. *R*-PIA prevented the downregulation of anti-apoptotic protein Bcl2 induced by cisplatin treatment. The figure shown is a representative of four similar experiments showing similar results.

regulated inflammatory pathways. To determine whether *R*-PIA prevented cisplatin-induced inflammation *in vivo*, we examined the levels of TNF-α in the cochlea by immunohistochemistry. High TNF-α immunolabeling was observed 3 d after administration of cisplatin in the SG and OHCs, but not in the SVA or SL, compared with vehicle-treated rats. Trans-tympanic administration of *R*-PIA suppressed the increases in the immunolabeling of TNF-α (Fig. 6*A*). *R*-PIA also suppressed cisplatin-induced TNF-α mRNA levels from whole cochlear RNA preparations. Cisplatin induced a ~3.1 ± 0.5 fold increase in the expression of *TNF-α* in the cochlea, and this was attenuated by trans-tympanic administration of *R*-PIA (0.37 ± 0.3 fold; Fig. 6*C*). Blockade of the A_1AR with DPCPX led to reversal of the anti-inflammatory effect of *R*-PIA and to potentiation of cisplatin-induced TNF-α immunolabeling in the SVA and SL (Fig. 6*A*,*B*,*D*). A similar pattern of changes was observed at the mRNA level (Fig. 6*C*). These data indicate that the OHCs and SG cells could produce cytokines (e.g., TNF-α) in response to cisplatin and that the production of these cytokines is under the control of A_1AR present on these cells. The finding that activation of the A_1AR reduced the levels of TNF-α from these various regions of the cochlea suggests that increases in TNF-α in these regions might contribute to the overall inflammation and hearing loss produced by cisplatin and also support previous findings that inhibition of TNF-α by etanercept reduced cisplatin-induced hearing loss (Kaur et al., 2011).

Activation of A_1AR attenuates cisplatin-mediated apoptosis

Treatment with cisplatin increases cochlear cell apoptosis (Mukherjea et al., 2008). We have shown previously that STAT1 is the key regulator of cisplatin-induced apoptosis both *in vitro* and *in vivo* by activating the classical apoptotic pathway directly (Kaur et al., 2011). Induction of apoptotic markers involves the Ser^{727} p-STAT1 instead of Tyr^{701} p-STAT1 phosphorylation (Stephanou et al., 2001). Results, described above, indicated that *R*-PIA targeted Ser^{727}, but not Tyr^{701}, for inhibition. Therefore, we investigated whether *R*-PIA also inhibits cisplatin-mediated apoptosis. UB/OC-1 cells were pretreated with *R*-PIA (1 μM) before cisplatin administration (20 μM) for 24 h. The percentage of apoptotic cells measured by Annexin V staining increased from ~9% for vehicle-treated cells to ~40% for cisplatin-treated

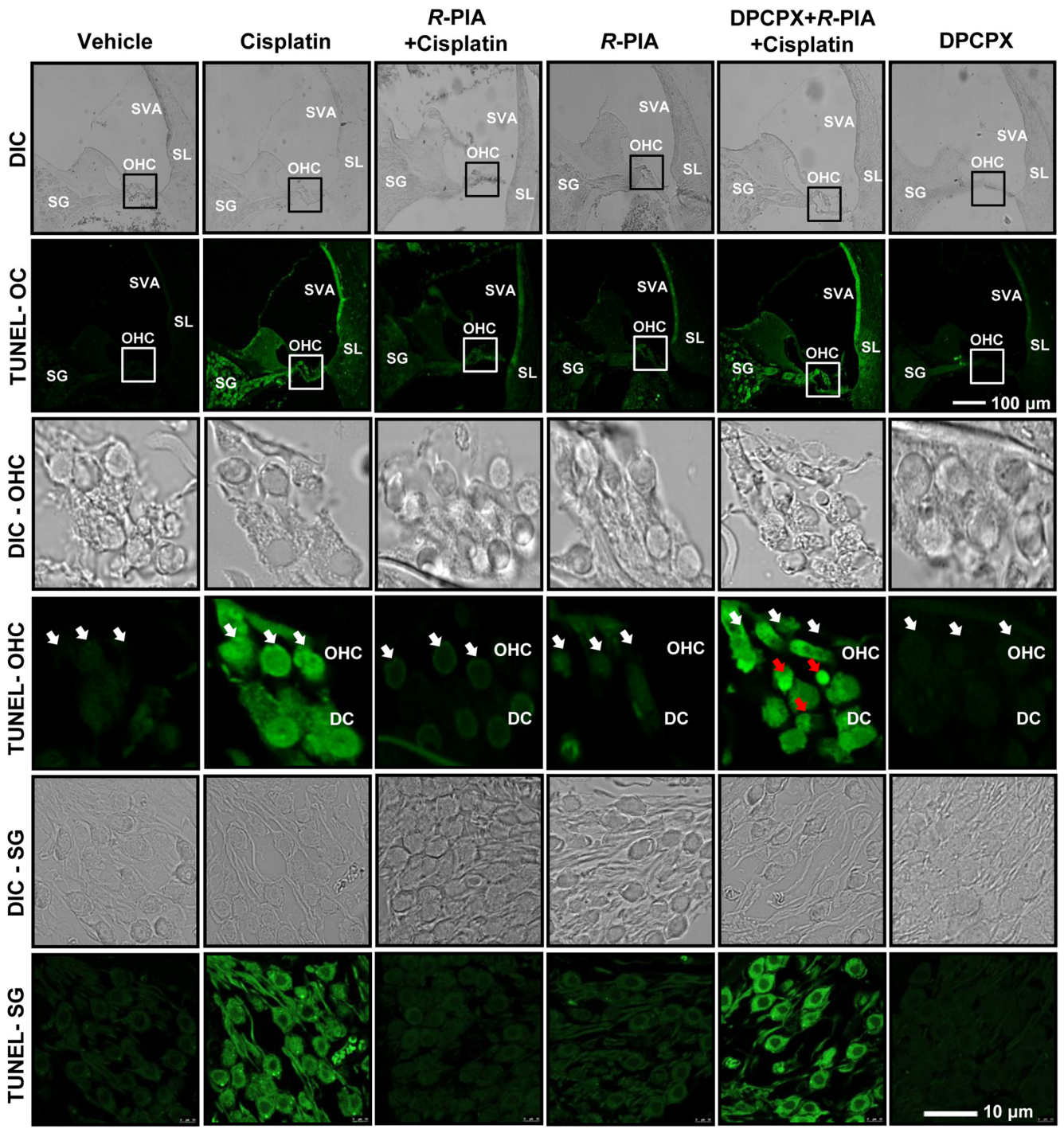

Figure 8. *R*-PIA reduced cisplatin-mediated apoptosis in the rat cochlea. TUNEL assay was performed on the cochlear section isolated from Wistar rats treated with trans-tympanic injection of *R*-PIA (1 μM) for 0.5 h, followed by vehicle or cisplatin (11 mg/kg) administration, and assessed 3 d later. Cisplatin increased the TUNEL-positive staining in the OHCs, Deiter' cells (DC), and SGs (see the higher magnification in the bottom). *R*-PIA pretreatment reduced the TUNEL-positive staining induced by cisplatin and DPCPX reversed the protective effect of *R*-PIA. DPCPX also produced nuclear fragmentation in OHCs and Deiter's cells from the cisplatin-treated cells rats (see red arrows). Top scale bar, 100 μm. Magnified view of the OHCs and SGs is presented in bottom three panels. White arrows indicate three rows of OHCs. Bottom scale bar, 10 μm.

cells. The increase in apoptosis produced by cisplatin was abolished by *R*-PIA (Fig. 7*A*,*B*). An interesting observation was that a larger percentage of UB/OC-1 cells that were Annexin V positive (apoptotic) expressed A_1AR than cells that were Annexin V negative (47 ± 3% of apoptotic cells vs 30 ± 2% of cells that were Annexin V negative). One explanation for these data is that cells that ultimately became apoptotic increased their output of A_1AR in a futile effort to survive compared with cells that survived cisplatin. These data also suggest that the levels of A_1AR on UB/OC-1 cells alone do not dictate the survival of these cells against cisplatin; rather, it is the activation of the A_1AR by agonist that was a key to survival.

Cisplatin-induced cleavage of pro-caspase 3 to caspase 3 was also abolished by *R*-PIA (Fig. 7*C*). Cells exposed to cisplatin showed reductions in Bcl2 that were inhibited by *R*-PIA (Fig. 7*C*). *R*-PIA also reduced cisplatin-induced p-53 induction (data not

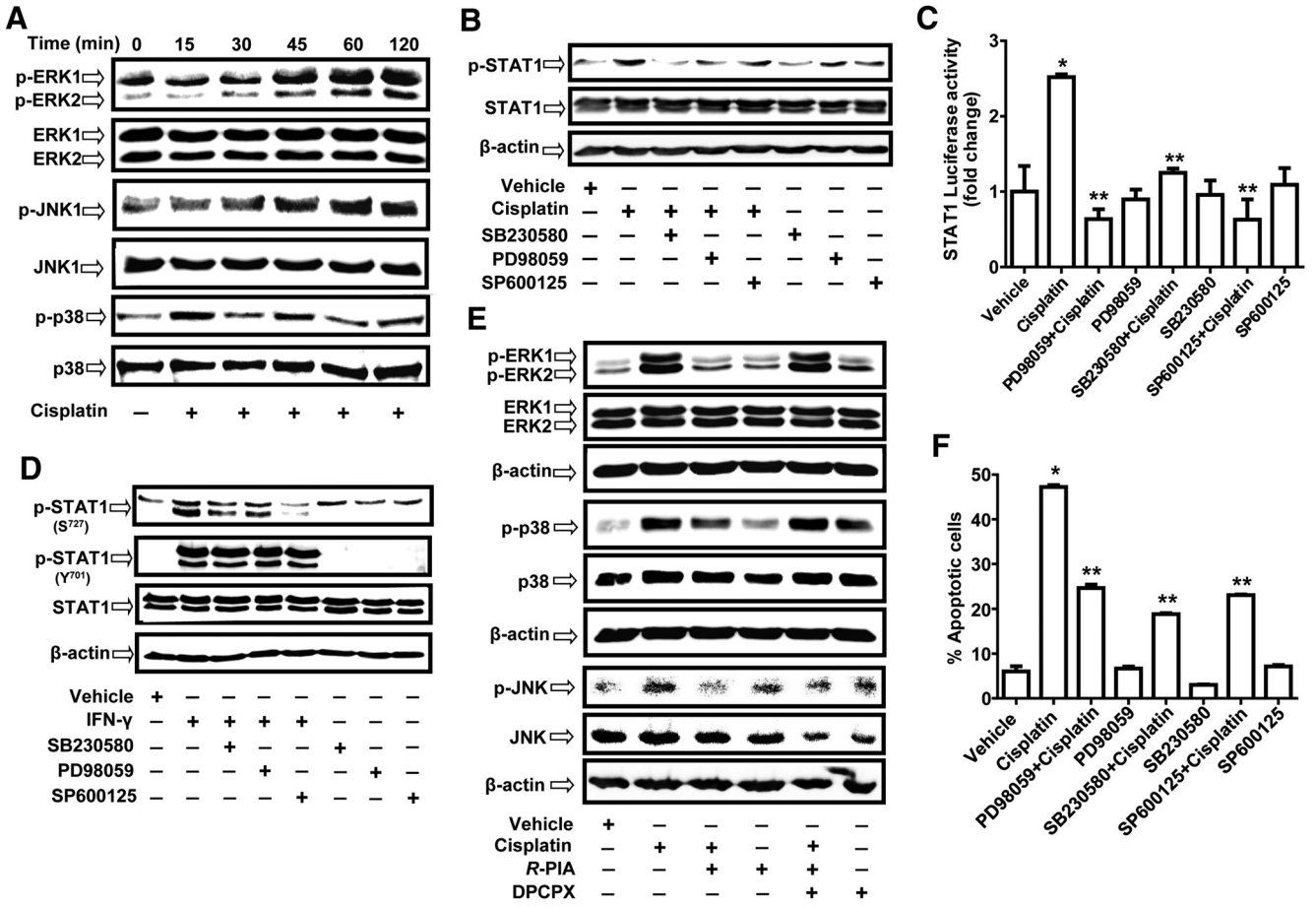

Figure 9. *R*-PIA inhibits STAT1 activity by decreasing MAPK activation. ***A***, UB/OC-1 cells were treated with cisplatin (2.5 μM) and the phosphorylation of ERK1/2, p38, and JNK1 were evaluated at 0, 15, 30, 45, 60, and 120 min. The respective phosphorylated MAPK was normalized to its total protein level. ***B***, The MAPK inhibitors SB230580, PD98059, and SP600125 reduced cisplatin-induced STAT1 phosphorylation. ***C***, MAPK inhibitors reduced cisplatin-induced STAT1 luciferase activity. Data are presented as the mean ± SEM of four experiments. *Statistically significant difference from control ($p < 0.05$); ** statistically significant difference from the cisplatin-treated group ($p < 0.05$). ***D***, MAPK inhibitors reduced the IFN-γ-activated Ser^{727} p-STAT1, but not Tyr^{701} STAT1 phosphorylation. ***E***, *R*-PIA inhibited cisplatin-induced activation of ERK1/2, p38, and JNK phosphorylation. ***F***, MAPK inhibitors reduced cisplatin-induced apoptosis of UB/OC-1 cells. Cells were treated with vehicle or 20 μM cisplatin or a combination of cisplatin + MAPK inhibitors. Results shown in ***A***, ***B***, ***D***, and ***E*** are each a representative of a single experiment that was replicated at least three times. Data are presented as the mean ± SEM of four experiments. *Statistically significant difference from control ($p < 0.05$); **statistically significant difference from cisplatin-treated group ($p < 0.05$).

shown) and prevented cisplatin-induced apoptosis in the organ of Corti of Wistar rats, as measured by TUNEL staining (Fig. 8). Cisplatin produced damage to the OHCs, SG, SL, and SVA, as depicted by green fluorescent staining, indicating TUNEL-positive cells. Trans-tympanic administration of *R*-PIA before cisplatin treatment reduced the number of TUNEL-positive cells in the respective areas of the organ of Corti mentioned above (Fig. 8). At higher magnification, intense Annexin–FITC labeling was observed in both OHCs and Deiter's cells. *R*-PIA-mediated protection against cisplatin apoptosis was abolished by DPCPX. Increased nuclear fragments were observed in OHCs and Deiter's cells stained in the cisplatin + DPCPX-treated cochleae compared with cisplatin-treated cochleae (Fig. 8, middle two panels). These data implicate the A_1AR in suppressing cisplatin-induced apoptotic of cochlear cells. The finding of greater nuclear damage induced by cisplatin in the presence of DPCPX suggests that the A_1AR provides some level of tonic suppression of apoptosis in the cochlea. Similar findings were observed in the SG neurons, in which cisplatin-increased apoptosis was blocked by *R*-PIA, whereas this protective action was abolished by DPCPX (Fig. 8, bottom three panels).

A_1AR reduces STAT1 activation by inhibition of MAPKs

Serine phosphorylation was first described for STAT1, STAT3, and STAT4 due to presence of a mitogen-activated protein kinase (MAPK) consensus sequence, PMSP, at the C-terminal tail at Ser^{727} for STAT1 (Zhang et al., 1995) and STAT3 (Wen et al., 1995). Phosphorylation of Ser^{727} STAT1 could be achieved by serine kinases such as the MAPKs, ERK 1/2 (David et al., 1995; Jain et al., 1998), p38 (Turkson et al., 1999; Zauberman et al., 1999), and JNK (Lim and Cao, 1999; Turkson et al., 1999). Phosphorylation could also be mediated by PKC-δ (Jain et al., 1999) or PKC-ε (Aziz et al., 2010). A number of studies have implicated ERK1/2 and p38 in cisplatin-mediated damage to the auditory hair cells (Wu et al., 2005; Previati et al., 2007; So et al., 2007; So et al., 2008; Abi-Hachem et al., 2010; Lee et al., 2010; Tabuchi et al., 2011). We therefore, hypothesized that cisplatin increases Ser^{727} p-STAT1 via the MAPK pathway. To test our hypothesis, we determined the effect of cisplatin on activation of MAPKs in UB/OC-1 cells. Cisplatin (2.5 μM) increased the activity of ERK1/2, JNK and p38. Phosphorylation of ERK 1/2 and JNK started 45 min following cisplatin administration and remained elevated up to 120 min, whereas p38 phosphorylation started

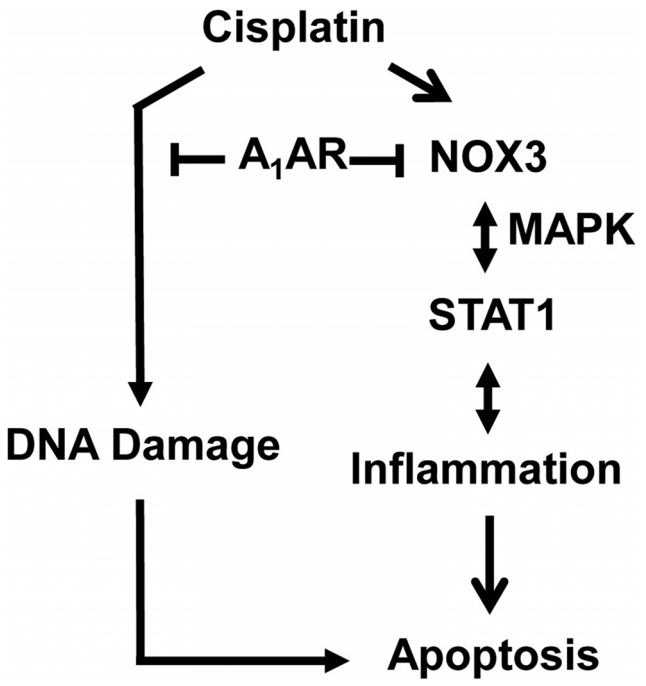

Figure 10. Proposed model of A_1AR protection against cisplatin-induced ototoxicity. Cisplatin activates and induces NOX3, which triggers MAPK and STAT1 activation. STAT1 increases cochlear inflammation (production of TNF-α, iNOS, and COX-2), which contributes to apoptosis. A_1AR reduction of cisplatin-induced apoptosis could also result from a direct reduction in DNA damage (as assessed by reduction in cleaved caspase).

within 15 min and remained elevated up to 45 min before returning to baseline (Fig. 9*A*). Pretreatment of UB/OC-1 cells with inhibitors of ERK 1/2 (PD98059), p38 (SB230580), and JNK (SP600125) reduced cisplatin increased Ser^{727} p-STAT1 levels (Fig. 9*B*). PD96059, SB230580 and SP600125 also reduced cisplatin-induced STAT1 luciferase activity in UB/OC-1 cells (Fig. 9*C*). Similar to the results with cisplatin, inhibition of ERK1/2, p38 and JNK reduced IFN-γ induced Ser^{727} but not Tyr^{701} p-STAT1 (Fig. 9*D*), suggesting that the MAPKs regulate mainly the Ser^{727} phosphorylation of STAT1. Furthermore, we show that *R*-PIA (1 μM) reduced cisplatin-mediated activation of ERK1/2, p38, and JNK. These effects were reversed by DPCPX, implicating A_1AR in these processes (Fig. 9*E*). Overall, these data suggest that the protective action of the A_1AR against cisplatin activation of STAT1 involves inhibition of the MAPK pathways. Additional studies were performed to determine whether MAPK inhibitors protect against cisplatin-induced apoptosis. Pretreatment of UB/OC-1 cells with SB230580 (10 μM), PD98059 (10 μM), or SP600125 (10 μM), followed by cisplatin (20 μM), led to significant reductions in apoptosis of UB/OC-1 cells. Cisplatin increased cell apoptosis to 47 $\pm$ 1%, whereas SB230580, PD98059, and SP600125 reduced the levels of apoptosis to 18.8 $\pm$ 0.2, 24.7 $\pm$ 0.8, and 23.1 $\pm$ 0.1%, respectively (Fig. 9*F*).

Discussion

The major finding of this study is that the A_1AR subserves an anti-inflammatory role in the cochlea that contributes to its ability to protect against cisplatin-induced hearing loss. This process primarily involves inhibition of ROS generation via NOX3 NADPH oxidase, which leads to inhibition of the STAT1 transcription factor and reduced expression of inflammatory mediators and pro-apoptotic proteins. Therefore, drugs that boost the levels of endogenous adenosine or activate the A_1AR directly could play a pivitol role in the survival of cells in the organ of Corti against cisplatin-mediated apoptosis. Therefore, the A_1AR could serve as an ideal target for otoprotective therapy against cisplatin-induced hearing loss.

The current study extends previous studies showing that activation of the A_1AR protects against cisplatin-induced ototoxicity in the chinchilla (Ford et al., 1997b) and rat (Whitworth et al., 2004). In the latter study, protection was mediated specifically via the A_1AR, without contribution from other AR subtypes. This specificity is likely linked to the expression pattern of ARs in the cochlea, with the A_1AR being the most abundant (Ramkumar et al., 1994). It has also been shown that the adenosine analog ADAC protected the cochlea against cisplatin-induced loss of OHCs and hearing loss (Gunewardene et al., 2013). The protective role of the A_1AR in the cochlea was reported to be due to its ability to increase antioxidant enzymes, leading to decreased lipid peroxidation (Ford et al., 1997a). This mechanism of protection appears quite plausible because administration of antioxidants reduces cisplatin ototoxicity (Rybak et al., 2007). The broader significance of a ROS hypothesis for mediating hearing loss was not completely appreciated at that time. However, our recent studies have provided a link between ROS generation and inflammation in the cochlea. We have shown that STAT1 couples ROS generation to cisplatin-induced inflammation in the cochlea (Mukherjea et al., 2011; Kaur et al., 2011). ROS mediate STAT1 Ser^{727} phosphorylation, but not Tyr^{701} phosphorylation (Kaur et al., 2011). Ser^{727} p-STAT1 interacts positively with p53 to enhance cell apoptosis. These studies clearly identified STAT1 as a critical factor in mediating cisplatin ototoxicity by regulating inflammatory and apoptotic processes. Accordingly, downregulation of STAT1 (by siRNA) or inhibition of TNF-α (by etanercept) protected against cisplatin-induced hearing loss (Kaur et al., 2011).

In the current study, we determined whether activation of the A_1AR regulates these cisplatin-induced ROS, inflammatory and apoptotic pathways. Our data identified NOX3 NADPH oxidase as a major target of inhibition by the A_1AR. The A_1AR inhibited NOX3 activity and reduced its expression, which could reduce the overall oxidative stress in the cochlea and highlight NOX3 as a novel target of the A_1AR. This finding is highly significant in light of the current therapeutic strategy to inhibit NOX3 by small molecules for treating hearing loss (Rybak et al., 2012; Rousset et al., 2015). We show that ROS stimulate MAPKs (ERK1/2, p38, and JNK), which activate Ser^{727} p-STAT1 and its transcriptional activity through distinct phosphorylation sites for ERK1/2 and p38 identified in the STAT1 protein sequence. These data suggest a specific role of Ser^{727} p-STAT1 in mediating cisplatin ototoxicity and as a target for the otoprotective action of the A_1AR. The localization of the A_1AR responsible for protection of OHCs against cisplatin-induced apoptosis is controversial. Previous studies indicated that the A_1AR is localized primarily to the IHCs, Deiter's cells, and SG neurons (Vlajkovic et al., 2009). We show the presence of A_1AR, albeit at lower levels, on OHCs. Therefore, it is reasonable to conclude that protection of OHCs and preservation of hearing is mediated, at least in part, through activation of A_1AR present on OHCs. However, it is possible protection of the OHCs is also mediated by A_1AR present on Deiter's cells, which also express A_1AR (Vlajkovic et al., 2009) through some intercellular processes. We observed that cisplatin increased the levels of TNF-α and apoptosis of Deiter's cells that were inhibited by activation of the A_1AR. Protection of Deiter's cells would lead indirectly to protection of OHCs (May et al., 2013). Cisplatin also

produced a global increase in TNF-α, which could contribute to the overall inflammatory stress experienced by the OHCs.

Although the OHCs were sensitive to cisplatin, the IHCs were relatively resistant to this drug (Nakai et al., 1982). We reasoned that the A1AR present on IHCs could contribute to their resistance to cisplatin. However, blockade of the A_1AR in neonatal organ of Corti explant cultures enhanced loss of OHCs, but did not affect the number of IHCs. Therefore, other mechanisms underlying resistance of IHCs to cisplatin have to be invoked. An interesting observation is that the IHCs express a high-affinity thiamine transporter, disruption of which leads to selective loss of these cells (Liberman et al., 2006). An accumulation of thiamine, a potential scavenger of cisplatin, into these cells might render them resistant to cisplatin. Lower levels of expression of *SLC19A2* in OHCs (Fleming et al., 2001) could render them less able to detoxify cisplatin and thus succumb to this drug. It is also possible that OHCs and IHCs express different platinum influx and efflux transporters that could regulate the steady-state drug levels.

Cisplatin-derived ROS increased the expression of the A_1AR by activating NF-κB (Nie et al., 1998), which could serve as a compensatory mechanism to reduce the toxicity of cisplatin. Other studies support a role of the ROS/NF-κB axis in the regulation of the A_1AR by oxidative stress (Pingle et al., 2004; Jajoo et al., 2006; Basheer et al., 2007; Pingle et al., 2007).

Localized trans-tympanic administration of *R*-PIA is needed for otoprotection to avoid potential systemic side effects of this drug. However, the recent observation that another A_1AR agonist, adenosine amine congener, is otoprotective when administered systemically could facilitate the testing of this latter agent for otoprotection in human (Vlajkovic et al., 2010; Gunewardene et al., 2013). Complications of using adenosine analogs systemically for treating cisplatin-induced hearing loss are predicted cardiovascular and CNS side effects, along with the possibility that these drugs could interfere with cisplatin chemotherapeutic efficacy. Previous studies indicate differing roles of the A_1AR in different cancers. Activation of the A_1AR suppresses CW2 human colon cancer growth (Saito et al., 2010), but promotes the growth of breast cancer cells (Mirza et al., 2005). These findings suggest limiting the systemic use of A_1AR drugs when patients are administered cancer chemotherapeutic drugs such as cisplatin.

In a previous study (Kaur et al., 2011), we observed intense staining for immune cell markers (such as TNF-α) in the SVA, OHCs, SG, and SL after cisplatin administration (Kaur et al., 2011). These data are somewhat different from the current findings, which show no statistically significant increase in TNF-α immunoreactivity in the SVA and SL induced by cisplatin. However, increases in TNF-α levels were observed after the administration of cisplatin with DPCPX to inhibit the A_1AR. One explanation for the difference is that the conclusion from the previous study was based on visual inspection of the different regions for TNF-α immunofluorescence, whereas the current findings are based on actual quantification of the immunofluroscence. Secretion of inflammatory cytokines cells in the SG cells, SVA, and SL could increase the overall TNF-α levels experienced by cells in the organ of Corti. The expression of these immune markers was reduced by A_1AR activation at these locations, suggesting a functional anti-inflammatory role of this receptor at these locations in the cochlea. In several experiments, we showed that the addition of the A_1AR antagonist DPCPX not only blocked the protective effects of the agonist, but also potentiated cisplatin-induced ototoxicity, implying an active role of the endogenous A_1AR signaling system in otoprotection. Certainly, this endogenous system is only partially effective against cisplatin-induced ototoxicity and requires exogenous agonist to become fully effective. However, such an endogenous system could be protective against lower levels of oxidative and inflammatory stressors.

An obvious limitation of our study is that the findings obtained in UB/OC-1 cultures, derived from an embryonic mouse hair cell precursor line, might not be relevant to the adult rat cochlea. However, in most cases, the biochemical findings observed in these studies using UB/OC-1 cultures matched those observed in the rat cochlea. This suggests that, within the scope of this study, the UB/OC-1 cells were a relevant *in vitro* model with which to study the cochlea.

In summary, the current data show that the cochlea expresses A_1AR, which mediates tonic suppression of oxidative, inflammatory, and apoptotic processes. Administration of an A_1AR agonist enhances the protective role of adenosine and protects against cisplatin ototoxicity by inhibiting the NOX3/STAT1 signaling pathway. Protection is conferred primarily through suppression of cochlear oxidative stress and inflammation, which could initiate apoptosis of OHCs. In addition, protection could also be mediated through regulation of DNA damage/repair processes that reduce apoptosis (Fig. 10). Therefore, we propose that localized delivery of A_1AR agonists could serve as effective adjuncts to cisplatin chemotherapy to reduce the high degree of hearing loss observed in cancer patients treated with this drug regimen.

References

Abi-Hachem RN, Zine A, Van De Water TR (2010) The injured cochlea as a target for inflammatory processes, initiation of cell death pathways and application of related otoprotectives strategies. Recent Pat CNS Drug Discov 5:147–163. CrossRef Medline

Aziz MH, Hafeez BB, Sand JM, Pierce DB, Aziz SW, Dreckschmidt NE, Verma AK (2010) Protein kinase Cvarepsilon mediates Stat3Ser727 phosphorylation, Stat3-regulated gene expression, and cell invasion in various human cancer cell lines through integration with MAPK cascade (RAF-1, MEK1/2, and ERK1/2). Oncogene 29:3100–3109. CrossRef Medline

Bánfi B, Malgrange B, Knisz J, Steger K, Dubois-Dauphin M, Krause KH (2004) NOX3, a superoxide-generating NADPH oxidase of the inner ear. J Biol Chem 279:46065–46072. CrossRef Medline

Basheer R, Bauer A, Elmenhorst D, Ramesh V, McCarley RW (2007) Sleep deprivation upregulates A1 adenosine receptors in the rat basal forebrain. Neuroreport 18:1895–1899. CrossRef Medline

Boison D (2006) Adenosine kinase, epilepsy and stroke: mechanisms and therapies. Trends Pharmacol Sci 27:652–658. CrossRef Medline

Bouma MG, Stad RK, van den Wildenberg FA, Buurman WA (1994) Differential regulatory effects of adenosine on cytokine release by activated human monocytes. J Immunol 153:4159–4168. Medline

Bryant GM, Barron SE, Norris CH, Guth PS (1987) Adenosine is a modulator of hair cell-afferent neurotransmission. Hear Res 30:231–237. CrossRef Medline

Cronstein BN (1994) Adenosine, an endogenous anti-inflammatory agent. J Appl Physiol 76:5–13. Medline

Daval JL, Von Lubitz DK, Deckert J, Redmond DJ, Marangos PJ (1989) Protective effect of cyclohexyladenosine on adenosine A1-receptors, guanine nucleotide and forskolin binding sites following transient brain ischemia: a quantitative autoradiographic study. Brain Res 491:212–226. CrossRef Medline

David M, Petricoin E 3rd, Benjamin C, Pine R, Weber MJ, Larner AC (1995) Requirement for MAPK (ERK2) activity in interferon alpha- and interferon beta-stimulated gene expression through STAT proteins. Science 269:1721–1723. CrossRef Medline

De Sarro G, De Sarro A, Meldrum BS (1991) Anticonvulsant action of 2-chloroadenosine injected focally into the inferior colliculus and substantia nigra. Eur J Pharmacol 194:145–152. CrossRef Medline

Fedele DE, Li T, Lan JQ, Fredholm BB, Boison D (2006) Adenosine A1 receptors are crucial in keeping an epileptic focus localized. Exp Neurol 200:184–190. CrossRef Medline

Fleming JC, Steinkamp MP, Kawatsuji R, Tartaglini E, Pinkus JL, Pinkus GS, Fleming MD, Neufeld EJ (2001) Characterization of murine high-affinity thiamine transporter, Slc19a2. Mol Genet Metab 74:273–280. CrossRef Medline

Ford MS, Maggirwar SB, Rybak LP, Whitworth C, Ramkumar V (1997a) Expression and function of adenosine receptors in the chinchilla cochlea. Hear Res 105:130–140. CrossRef Medline

Ford MS, Nie Z, Whitworth C, Rybak LP, Ramkumar V (1997b) Up-regulation of adenosine receptors in the cochlea by cisplatin. Hear Res 111:143–152. CrossRef Medline

Fredholm BB, IJzerman AP, Jacobson KA, Linden J, Müller CE (2011) International Union of Basic and Clinical Pharmacology. LXXXI. Nomenclature and classification of adenosine receptors–an update. Pharmacol Rev 63:1–34. CrossRef Medline

Fujioka M, Kanzaki S, Okano HJ, Masuda M, Ogawa K, Okano H (2006) Proinflammatory cytokines expression in noise-induced damaged cochlea. J Neurosci Res 83:575–583. CrossRef Medline

Gunewardene N, Guo CX, Wong ACY, Thorne PR, Vlajkovic SM (2013) Adenosine amine congener ameliorates cisplatin-induced hearing loss. World Journal of Otorhinolaryngology 3:100–107. CrossRef

Haskó G, Szabó C, Németh ZH, Kvetan V, Pastores SM, Vizi ES (1996) Adenosine receptor agonists differentially regulate IL-10, TNF-alpha, and nitric oxide production in RAW 264.7 macrophages and in endotoxemic mice. J Immunol 157:4634–4640. Medline

Hight NG, McFadden SL, Henderson D, Burkard RF, Nicotera T (2003) Noise-induced hearing loss in chinchillas pre-treated with glutathione monoethylester and *R*-PIA. Hear Res 179:21–32. CrossRef Medline

Hu BH, Zheng XY, McFadden SL, Kopke RD, Henderson D (1997) R-phenylisopropyladenosine attenuates noise-induced hearing loss in the chinchilla. Hear Res 113:198–206. CrossRef Medline

Jain N, Zhang T, Fong SL, Lim CP, Cao X (1998) Repression of Stat3 activity by activation of mitogen-activated protein kinase (MAPK). Oncogene 17:3157–3167. CrossRef Medline

Jain N, Zhang T, Kee WH, Li W, Cao X (1999) Protein kinase C delta associates with and phosphorylates Stat3 in an interleukin-6-dependent manner. J Biol Chem 274:24392–24400. CrossRef Medline

Jajoo S, Mukherjea D, Pingle S, Sekino Y, Ramkumar V (2006) Induction of adenosine A1 receptor expression by pertussis toxin via an adenosine 5′-diphosphate ribosylation-independent pathway. J Pharmacol Exp Ther 317:1–10. Medline

Jajoo S, Mukherjea D, Watabe K, Ramkumar V (2009) Adenosine A(3) receptor suppresses prostate cancer metastasis by inhibiting NADPH oxidase activity. Neoplasia 11:1132–1145. CrossRef Medline

Kaur T, Mukherjea D, Sheehan K, Jajoo S, Rybak LP, Ramkumar V (2011) Short interfering RNA against STAT1 attenuates cisplatin-induced ototoxicity in the rat by suppressing inflammation. Cell Death Dis 2:e180. CrossRef Medline

Kochanek PM, Vagni VA, Janesko KL, Washington CB, Crumrine PK, Garman RH, Jenkins LW, Clark RS, Homanics GE, Dixon CE, Schnermann J, Jackson EK (2006) Adenosine A1 receptor knockout mice develop lethal status epilepticus after experimental traumatic brain injury. J Cereb Blood Flow Metab 26:565–575. CrossRef Medline

Lankford AR, Yang JN, Rose'Meyer R, French BA, Matherne GP, Fredholm BB, Yang Z (2006) Effect of modulating cardiac A1 adenosine receptor expression on protection with ischemic preconditioning. Am J Physiol Heart Circ Physiol 290:H1469–1473. Medline

Lee JS, Kang SU, Hwang HS, Pyun JH, Choung YH, Kim CH (2010) Epicatechin protects the auditory organ by attenuating cisplatin-induced ototoxicity through inhibition of ERK. Toxicol Lett 199:308–316. CrossRef Medline

Liberman MC, Tartaglini E, Fleming JC, Neufeld EJ (2006) Deletion of SLC19A2, the high affinity thiamine transporter causes selective inner hair cell loss and an auditory neuropathy phenotype. JARO 7:211–217. CrossRef Medline

Lim CP, Cao X (1999) Serine phosphorylation and negative regulation of Stat3 by JNK. J Biol Chem 274:31055–31061. CrossRef Medline

May LA, Kramarenko II, Brandon CS, Voelkel-Johnson C, Roy S, Truong K, Francis SP, Monzack EL, Lee FS, Cunningham LL (2013) Inner ear supporting cells protect hair cells by secreting HSP70. J Clin Invest 123:3577–3587. CrossRef Medline

Merchant SN, Gopen Q (1996) A human temporal bone study of acute bacterial meningogenic labyrinthitis. Am J Otol 17:375–385. Medline

Mirza A, Basso A, Black S, Malkowski M, Kwee L, Pachter JA, Lachowicz JE, Wang Y, Liu S (2005) RNA interference targeting of A1 receptor-expressing breast carcinoma cells leads to diminished rates of cell proliferation and induction of apoptosis. Cancer Bio Ther 4:1355–1360. CrossRef

Mukherjea D, Jajoo S, Whitworth C, Bunch JR, Turner JG, Rybak LP, Ramkumar V (2008) Short interfering RNA against transient receptor potential vanilloid 1 attenuates cisplatin-induced hearing loss in the rat. J Neurosci 28:13056–13065. CrossRef Medline

Mukherjea D, Jajoo S, Kaur T, Sheehan KE, Ramkumar V, Rybak LP (2010) Transtympanic administration of short interfering (si)RNA for the NOX3 isoform of NADPH oxidase protects against cisplatin-induced hearing loss in the rat. Antioxid Redox Signal 13:589–598. CrossRef Medline

Mukherjea D, Jajoo S, Sheehan K, Kaur T, Sheth S, Bunch J, Perro C, Rybak LP, Ramkumar V (2011) NOX3 NADPH oxidase couples transient receptor potential vanilloid 1 to signal transducer and activator of transcription 1-mediated inflammation and hearing loss. Antioxid Redox Signal 14:999–1010. CrossRef Medline

Nakai Y, Konishi K, Chang KC, Ohashi K, Morisaki N, Minowa Y, Morimoto A (1982) Ototoxicity of the anticancer drug cisplatin: an experimental study. Acta Oto-laryngologica 93:227–232. CrossRef Medline

Nario K, Kitano I, Mori N, Matsunaga T (1994) The effect of adenosine on cochlear potentials in the guinea pig. Eur Arch Otorhinolaryngol 251:428–433. Medline

Nie Z, Mei Y, Ford M, Rybak L, Marcuzzi A, Ren H, Stiles GL, Ramkumar V (1998) Oxidative stress increases A1 adenosine receptor expression by activating nuclear factor kappa B. Mol Pharmacol 53:663–669. Medline

Paparella MM, Oda M, Hiraide F, Brady D (1972) Pathology of sensorineural hearing loss in otitis media. Ann Otol Rhinol Laryngol 81:632–647. CrossRef Medline

Pingle SC, Mishra S, Marcuzzi A, Bhat SG, Sekino Y, Rybak LP, Ramkumar V (2004) Osmotic diuretics induce adenosine A1 receptor expression and protect renal proximal tubular epithelial cells against cisplatin-mediated apoptosis. J Biol Chem 279:43157–43167. CrossRef Medline

Pingle SC, Jajoo S, Mukherjea D, Sniderhan LF, Jhaveri KA, Marcuzzi A, Rybak LP, Maggirwar SB, Ramkumar V (2007) Activation of the adenosine A1 receptor inhibits HIV-1 tat-induced apoptosis by reducing nuclear factor-kappaB activation and inducible nitric-oxide synthase. Mol Pharmacol 72:856–867. CrossRef Medline

Previati M, Lanzoni I, Astolfi L, Fagioli F, Vecchiati G, Pagnoni A, Martini A, Capitani S (2007) Cisplatin cytotoxicity in organ of Corti-derived immortalized cells. J Cell Biochem 101:1185–1197. CrossRef Medline

Puntambekar P, Van Buren J, Raisinghani M, Premkumar LS, Ramkumar V (2004) Direct interaction of adenosine with the TRPV1 channel protein. J Neurosci 24:3663–3671. CrossRef Medline

Ramkumar V, Ravi R, Wilson MC, Gettys TW, Whitworth C, Rybak LP (1994) Identification of A1 adenosine receptors in rat cochlea coupled to inhibition of adenylyl cyclase. Am J Physiol 267:C731–737. Medline

Ribeiro L, Azevedo I, Martel F (2002) Comparison of the effect of cyclic AMP on the content and release of dopamine and 1-methyl-4-phenylpyridinium (Mpp+) in PC12 cells. Auton Autacoid Pharmacol 22:277–289. CrossRef Medline

Rivolta MN, Grix N, Lawlor P, Ashmore JF, Jagger DJ, Holley MC (1998) Auditory hair cell precursors immortalized from the mammalian ear. Proc Biol Sci 265:1595–1603. CrossRef Medline

Rousset F, Carnesecchi S, Senn P, Krause KH (2015) NOX3 targeted therapies for inner ear pathologies. Curr Pharm Des 21:5977–5987. CrossRef Medline

Rudolphi KA, Keil M, Fastbom J, Fredholm BB (1989) Ischaemic damage in gerbil hippocampus is reduced following upregulation of adenosine (A1) receptors by caffeine treatment. Neurosci Lett 103:275–280. CrossRef Medline

Rudolphi KA, Schubert P, Parkinson FE, Fredholm BB (1992) Adenosine and brain ischemia. Cerebrovasc Brain Metab Rev 4:346–369. Medline

Rybak LP, Whitworth CA, Mukherjea D, Ramkumar V (2007) Mechanisms of cisplatin-induced ototoxicity and prevention. Hear Res 226:157–167. CrossRef Medline

Rybak LP, Mukherjea D, Jajoo S, Kaur T, Ramkumar V (2012) siRNA-mediated knock-down of NOX3:therapy for hearing loss? Cell Mol Life Sci 69:2429–2434. CrossRef Medline

Saito M, Yaguchi T, Yasuda Y, Nakano T, Nishizaki T (2010) Adenosine

suppresses CW2 human colonic cancer growth by inducing apoptosis via A(1) adenosine receptors. Cancer Lett 290:211–215. CrossRef Medline

Sajjadi FG, Takabayashi K, Foster AC, Domingo RC, Firestein GS (1996) Inhibition of TNF-alpha expression by adenosine: role of A3 adenosine receptors. J Immunol 156:3435–3442. Medline

Schmitt NC, Rubel EW, Nathanson NM (2009) Cisplatin-induced hair cell death requires STAT1 and is attenuated by epigallocatechin gallate. J Neurosci 29:3843–3851. CrossRef Medline

Schulte G, Sommerschild H, Yang J, Tokuno S, Goiny M, Lövdahl C, Johansson B, Fredholm BB, Valen G (2004) Adenosine A receptors are necessary for protection of the murine heart by remote, delayed adaptation to ischaemia. Acta Physiol Scand 182:133–143. CrossRef Medline

Simon AR, Rai U, Fanburg BL, Cochran BH (1998) Activation of the JAK-STAT pathway by reactive oxygen species. Am J Physiol 275:C1640–C1652. Medline

So H, Kim H, Lee JH, Park C, Kim Y, Kim E, Kim JK, Yun KJ, Lee KM, Lee HY, Moon SK, Lim DJ, Park R (2007) Cisplatin cytotoxicity of auditory cells requires secretions of proinflammatory cytokines via activation of ERK and NF-kappaB. J Assoc Res Otolaryngol 8:338–355. CrossRef Medline

So H, Kim H, Kim Y, Kim E, Pae HO, Chung HT, Kim HJ, Kwon KB, Lee KM, Lee HY, Moon SK, Park R (2008) Evidence that cisplatin-induced auditory damage is attenuated by downregulation of pro-inflammatory cytokines via Nrf2/HO-1. J Assoc Res Otolaryngol 9:290–306. CrossRef Medline

Soong R, Beyser K, Basten O, Kalbe A, Rueschoff J, Tabiti K (2001) Quantitative reverse transcription-polymerase chain reaction detection of cytokeratin 20 in noncolorectal lymph nodes. Clin Cancer Res 7:3423–3429. Medline

Stephanou A, Scarabelli TM, Brar BK, Nakanishi Y, Matsumura M, Knight RA, Latchman DS (2001) Induction of apoptosis and Fas receptor/Fas ligand expression by ischemia/reperfusion in cardiac myocytes requires serine 727 of the STAT-1 transcription factor but not tyrosine 701. J Biol Chem 276:28340–28347. CrossRef Medline

Tabuchi K, Nishimura B, Nakamagoe M, Hayashi K, Nakayama M, Hara A (2011) Ototoxicity: mechanisms of cochlear impairment and its prevention. Curr Med Chem 18:4866–4871. CrossRef Medline

Tsutsui S, Schnermann J, Noorbakhsh F, Henry S, Yong VW, Winston BW, Warren K, Power C (2004) A1 adenosine receptor upregulation and activation attenuates neuroinflammation and demyelination in a model of multiple sclerosis. J Neurosci 24:1521–1529. CrossRef Medline

Turkson J, Bowman T, Adnane J, Zhang Y, Djeu JY, Sekharam M, Frank DA, Holzman LB, Wu J, Sebti S, Jove R (1999) Requirement for Ras/Rac1-mediated p38 and c-Jun N-terminal kinase signaling in Stat3 transcriptional activity induced by the Src oncoprotein. Mol Cell Biol 19:7519–7528. CrossRef Medline

Vlajkovic SM, Abi S, Wang CJ, Housley GD, Thorne PR (2007) Differential distribution of adenosine receptors in rat cochlea. Cell Tissue Res 328:461–471. CrossRef Medline

Vlajkovic SM, Housley GD, Thorne PR (2009) Adenosine and the auditory system. Curr Neuropharmacol 7:246–256. CrossRef Medline

Vlajkovic SM, Lee KH, Wong AC, Guo CX, Gupta R, Housley GD, Thorne PR (2010) Adenosine amine congener mitigates noise-induced cochlear injury. Purinergic Signal 6:273–281. CrossRef Medline

Vlajkovic SM, Guo CX, Telang R, Wong AC, Paramananthasivam V, Boison D, Housley GD, Thorne PR (2011) Adenosine kinase inhibition in the cochlea delays the onset of age-related hearing loss. Exp Gerontol 46:905–914. CrossRef Medline

Von Lubitz DK, Lin RC, Melman N, Ji XD, Carter MF, Jacobson KA (1994) Chronic administration of selective adenosine A1 receptor agonist or antagonist in cerebral ischemia. Eur J Pharmacol 256:161–167. CrossRef Medline

Wen Z, Zhong Z, Darnell JE Jr (1995) Maximal activation of transcription by Stat1 and Stat3 requires both tyrosine and serine phosphorylation. Cell 82:241–250. CrossRef Medline

Whitworth CA, Ramkumar V, Jones B, Tsukasaki N, Rybak LP (2004) Protection against cisplatin ototoxicity by adenosine agonists. Biochem Pharmacol 67:1801–1807. CrossRef Medline

Wu YJ, Muldoon LL, Neuwelt EA (2005) The chemoprotective agent N-acetylcysteine blocks cisplatin-induced apoptosis through caspase signaling pathway. J Pharmacol Exp Ther 312:424–431. Medline

Zauberman A, Zipori D, Krupsky M, Ben-Levy R (1999) Stress activated protein kinase p38 is involved in IL-6 induced transcriptional activation of STAT3. Oncogene 18:3886–3893. CrossRef Medline

Zhang X, Blenis J, Li HC, Schindler C, Chen-Kiang S (1995) Requirement of serine phosphorylation for formation of STAT-promoter complexes. Science 267:1990–1994. CrossRef Medline